

Generalized Chaplygin Gas Models tested with SNIa

MAREK BIESIADA

Department of Astrophysics and Cosmology,

University of Silesia

Uniwersytecka 4, 40-007 Katowice, Poland

mb@imp.sosnowiec.pl

WŁODZIMIERZ GODŁOWSKI

Astronomical Observatory

Jagiellonian University

Orla171, Krakow, Poland

godlows@oa.uj.edu.pl

MAREK SZYDŁOWSKI

Astronomical Observatory

Jagiellonian University

Orla171, Krakow, Poland

szydlo@oa.uj.edu.pl

ABSTRACT

The Generalized Chaplygin Gas (GCG) with the equation of state $p = -\frac{A}{\rho^\alpha}$ was recently proposed as a candidate for dark energy in the Universe. In this paper we confront the GCG with SNIa data using available samples. Specifically we have tested the GCG cosmology in three different classes of models with (1) $\Omega_m = 0.3$, $\Omega_{Ch} = 0.7$; (2) $\Omega_m = 0.05$, $\Omega_{Ch} = 0.95$ and (3) $\Omega_m = 0$, $\Omega_{Ch} = 1$, as well as a model without prior assumptions on Ω_m . The best fitted models are obtained by minimalizing the χ^2 function. We supplement our analysis with confidence intervals in the (A_0, α) plane by marginalizing the probability density functions over remaining parameters assuming uniform priors. We have also derived one-dimensional probability distribution functions for Ω_{Ch} obtained from joint marginalization over α and A_0 . The maximum value of such PDF provides the most probable value of Ω_{Ch} within the full class of GCG models. The general conclusion is that SNIa data give support to the Chaplygin gas (with $\alpha = 1$). However noticeable preference of A_0 values close to 1 means that the α dependence becomes insignificant. It is reflected on one dimensional PDFs for α which turned out to be flat meaning that the power of present supernovae data to discriminate between various GCG models (differing by α) is weak. Extending our analysis by relaxing the prior assumption of the flatness of the Universe leads to

the result that even though the best fitted values of Ω_k are formally non-zero, still they are close to the flat case. Our results show clearly that in GCG cosmology distant (i.e. $z > 1$) supernovae should be brighter than in Λ CDM model. Therefore one can expect that future supernova experiments (e.g., SNAP) having access to higher redshifts will eventually resolve the issue whether the dark energy content of the Universe could be described as a the Chaplygin gas. Moreover, it would be possible to differentiate between models with various value of α parameter and/or discriminated between GCG, Cardassian and Λ CDM models. This discriminative power of the forthcoming mission has been demonstrated on simulated SNAP data.

Subject headings: cosmology:theory — distance scale —supernovae: Generalized Chaplygin Gas

1. Introduction

For a couple of years two independent observational programs — the high redshift supernovae surveys (Perlmutter et al. 1999) and CMBR small scale anisotropy measurements (de Bernardis et al. 2000, Benoit et al. 2003, Hinshaw et al. 2003) have brought a new picture of the Universe in the large. While interpreted within the FRW models results of these programs suggest that our Universe is flat (as inferred from the location of acoustic peaks in CMBR power spectrum) and presently accelerates its expansion (as inferred from the SNIa Hubble diagram). Combined with the independent knowledge about the amount of baryons and CDM estimated to be $\Omega_m = 0.3$ (Turner 2002) it follows that about $\Omega_X = 0.7$ fraction of critical density $\rho_{cr} = \frac{3c^2 H_0^2}{8\pi G}$ should be contained in a mysterious component called “dark energy”. The most obvious candidate for this smooth component permeating the Universe is the cosmological constant Λ representing the energy of the vacuum. Well known fine tuning problems led many people to seek beyond the Λ framework, and the concept of the quintessence had been conceived. Usually the quintessence is described in a phenomenological manner, as a scalar field with an appropriate potential (Ratra & Peebles 1988, Caldwell, Dave & Steinhardt 1995, Frieman, Stebbins & Waga 1995). It turns out, however, that quintessence program also suffers from its own fine tuning problems (Kolda & Lyth 1999).

In 1904 Russian physicist Chaplygin introduced the exotic equation of state $p = -\frac{A}{\rho}$ to describe an adiabatic aerodynamic process (Chaplygin 2004). The attractiveness of this equation of state in the context dark energy models comes mainly from the fact that it gives the unification of both dark energy (postulated in cosmology to explain current acceleration

of the Universe) and clustered dark matter which is postulated in astrophysics to explain the flat rotation curves of spiral galaxies. It is interesting that the Chaplygin gas can be derived from the quintessence Lagrangian for the scalar field ϕ with some potential and also from the Born-Infeld form of the Lagrangian (Kamenshchik, Moschella & Pasquier 2001). The Chaplygin equation of state has some interesting connections with string theory and it admits the interpretation in the framework of brane cosmologies (Jackiw 2000).

Recently the so called Chaplygin gas (Kamenshchik, Moschella & Pasquier 2001, Fabris, Gonçalves & de Souza 2002, Szydlowski & Czaja 2004) — a hypothetical component with the equation of state $p = -\frac{A}{\rho}$ — was proposed as a challenge to the above mentioned candidates for dark energy. This, also purely phenomenological, entity has interesting connections with string theory (Ogawa 2000). Currently its generalizations admitting the equation of state $p = -\frac{A}{\rho^\alpha}$ where $0 \leq \alpha \leq 1$ have been proposed (Bento, Bertolami & Sen 2002, Carturan & Finelli 2002a).

In this paper we confront the Generalized Chaplygin Gas with the SNIa data. At this point our choice of Generalized Chaplygin Gas cosmologies deserves a sort of justification. There are two approaches in the literature. First one is phenomenological, namely having no preferred theory of dark energy responsible for acceleration of the Universe one characterizes it as a cosmic fluid with an equation of state $p_X = w\rho_X$ where $w \geq -1$ (see e.g. (Chiba 1998, Turner & White 1997) and an immense literature that appeared thereafter). Because, as already mentioned above, a strain of ideas about dark energy is associated with an evolving scalar there are good reasons to expect that cosmic equation of state could be time dependent i.e. $w = w(t) = w(z)$ (e.g. Weller & Albrecht 2001, Maor et al. 2001 and many others thereafter). This approach seems attractive from the perspective of analyzing observational data such like supernovae surveys and indeed this approach was taken while first analyzing the data (Perlmutter et al. 1999, Knop et al. 2003 or Riess et al. 2004). However even though such analysis places constraints on *any* potential theory that might explain the dark energy phenomenon, ultimately one always ends up at testing a *specific* theory. Along this line there appeared attempts to reconstruct the scalar potential, if the scalar field was responsible for dark energy (e.g. Alam et al. 2003 and references therein). Our approach goes along this philosophy but instead is devoted to the Generalized Chaplygin Gas which is being recently considered as candidate to unified dark matter-energy component (i.e. responsible for both clustering and accelerated expansion (Makler, de Oliveira & Waga 2003)).

The cosmological models with the Generalized Chaplygin Gas have also many special features which make them attractive. In standard cosmological model one can clearly distinguish the epochs of radiation domination followed by (ordinary) matter domination (with decelerated expansion). As mentioned above supernova data suggest that the epoch of de-

celerated expansion ended and switched to accelerated epoch — dominated by dark energy. The Generalized Chaplygin Gas models describe smoothly the transition from the decelerated to accelerated epochs. They represent the simplest deformation of concordance Λ CDM (Gorini et al. 2004). And moreover, they propose a new unified macroscopic (phenomenological) description of both dark energy and dark matter. This places them in a distinguished position from the point of view of Occam’s razor principle. It should be also noted that the Generalized Chaplygin Gas model allowed us to explain presently observed acceleration of the Universe without the cosmological constant and/or modification of Einstein’s equations.

If one takes seriously given dark energy scenario (necessary to explain cosmic acceleration) one should also consider the behaviour of perturbations in such a universe. In the framework of quintessence models with the barotropic equation of state (i.e. $p = w\rho$ and $w = \text{const}$) one faces the problem of instabilities in short scales. This appears because the speed of sound squared (equal here to w) is negative (and constant). Calculation of the sound speed in Generalized Chaplygin Gas model (see below) reveal its non-barotropic nature. The perturbations in GCG models are stable in short scales even in an accelerating phase (Carturan & Finelli 2002a). Moreover, they behave like dust perturbations when Chaplygin Gas is in dust regime.

Another motivation for studying Generalized Chaplygin Gas models goes from theoretical physics — specifically from attempts to describe the dark energy in terms of the Lagrangian for a tachyonic field (Garousi 2000, Sen 2002). Of course it would be nice to have a description of dark energy in terms of the non quintessence Lagrangian as it describes the nature of dark energy while the cosmological constant is only phenomenological and effective description. One should also note that the Generalized Chaplygin Gas equation of state arises in modern physics in the context of brane models (Bordemann & Hoppe 1993, Kamenshchik, Moschella & Pasquier 2001, Randall & Sundrum 1999) where the Generalized Chaplygin Gas manifests itself as an effect of immersion of our Universe in multidimensional bulk space.

Generalized Chaplygin gas models have been intensively studied in the literature and in particular they have been tested against supernovae data (Makler, de Oliveira & Waga 2003, Avelino et al. 2003, Collistete et al. 2003), lensing statistics (Dev, Alcaniz & Jain 2003), CMBR measurements (Bento, Bertolami & Sen 2003a, 2003b, Carturan & Finelli 2003b, Amendola et al. 2003), age-redshift relation (Alcaniz, Jain & Dev 2003), x-ray luminosities of galaxy clusters (Cunha, Lima & Alcaniz 2003) or from the large scale structure considerations (Bean & Doré 2003, Multamaki, Manera & Gaztanaga 2003, Bilic et al. 2003). Perspectives to distinguish between Generalized Chaplygin Gas, brane-world scenarios and quintessence in forthcoming gravity wave experiments has been discussed in (Biesiada 2003). Although

the results are in general mutually consistent there was no strong convergence to unique values of A_0 , α parameters characterizing Chaplygin gas equation of state.

Makler, de Oliveira & Waga (2003) have considered the FRW model filled completely with Generalized Chaplygin Gas and concluded that whole class of such models is consistent with current SNIa data although the value of $\alpha = 0.4$ is favoured. This result has been confirmed by our analysis (class (3) models). However, when the existing knowledge about baryonic matter content of the Universe was incorporated into the study our results were different from Makler, de Oliveira & Waga (2003) who found that $\alpha = 0.15$ was preferred (assuming $\Omega_m = 0.04$ which is very close to our assumption for class (2) models).

As noticed by Bean & Doré (2003) Generalized Chaplygin Gas models have an inherent degeneracy with cosmological constant models as far as background evolution is concerned, and therefore they have a good fit with SNIa data. These degeneracies disappear at the level of evolution of perturbations and hence confrontation with CMBR spectrum would be decisive. Using available data on the position of CMBR peaks measured by BOOMERANG (de Bernardis et al. 2000) and Archeops (Benoit et al. 2003, Hinshaw et al. 2003, Bento, Bertolami & Sen (2002) obtained the following constraints: $0.81 \leq A_0 \leq 0.85$ and $0.2 \leq \alpha \leq 0.6$ at 68% CL in the model representative of our class (2) (i.e. with $\Omega_m = 0.05$ assumed). Another estimation of the parameter α was done by Amendola et al. (2003) with WMAP Data. The obtained the $0 \leq \alpha < 0.2$ at 95% confidence level.

Using the angular size statistics for extragalactic sources combined with SNIa data it was found in (Alcaniz & Lima 2003) that in the the $\Omega_m = 0.3$ and $\Omega_{Ch} = 0.7$ scenario best fitted values of model parameters are $A_0 = 0.83$ and $\alpha = 1$. respectively. Recent paper by Bertolami et al. (2004) in which Generalized Chaplygin Gas models have been analyzed against Tonry et al. (2003) supernovae data relaxing the prior assumption on flatness suggests, surprisingly as the authors admit, the preference of $\alpha > 1$.

Table 1. Results of statistical analysis of Generalized Chaplygin Gas model (with marginalization over \mathcal{M}) performed on analyzed samples of SNIA (A, C, K6, K3, TBI, TBII, Silver, Gold) as a minimum χ^2 best-fit (denoted BF) and with the maximum likelihood method (denoted L). First two rows for each sample refer to no prior on Ω_m . The same analysis was repeated with fixed priors $\Omega_m = 0.0$, $\Omega_m = 0.05$ and $\Omega_m = 0.3$.

sample	Ω_m	Ω_{Ch}	A_0	α	\mathcal{M}	χ^2	method
A	0.00	1.00	0.77	1.00	-3.39	95.4	BF
	0.17	0.83	0.83	0.00	-3.36	—	L
	0.00	1.00	0.77	1.00	-3.39	95.4	BF
	0.00	1.00	0.73	1.00	-3.38	—	L
	0.05	0.95	0.80	1.00	-3.39	95.4	BF
	0.05	0.95	0.76	1.00	-3.38	—	L
	0.30	0.70	0.96	1.00	-3.39	95.8	BF
	0.30	0.70	0.96	0.00	-3.38	—	L
C	0.00	1.00	0.80	1.00	-3.44	52.9	BF
	0.15	0.85	0.86	0.00	-3.41	—	L
	0.00	1.00	0.80	1.00	-3.44	52.9	BF
	0.00	1.00	0.76	0.49	-3.43	—	L
	0.05	0.95	0.83	1.00	-3.44	53.0	BF
	0.05	0.95	0.79	0.11	-3.43	—	L
	0.30	0.70	0.99	1.00	-3.42	53.3	BF
	0.30	0.70	0.99	0.00	-3.39	—	L
K6	0.00	1.00	0.81	1.00	-3.52	55.3	BF
	0.10	0.90	0.88	0.00	-3.51	—	L
	0.00	1.00	0.81	1.00	-3.52	55.3	BF
	0.00	1.00	0.78	0.71	-3.52	—	L
	0.05	0.95	0.84	1.00	-3.52	55.4	BF
	0.05	0.95	0.81	0.06	-3.52	—	L
	0.30	0.70	1.00	1.00	-3.51	55.9	BF
	0.30	0.70	1.00	0.00	-3.49	—	L
K3	0.00	1.00	0.85	1.00	-3.48	60.4	BF
	0.11	0.89	0.88	0.00	-3.45	—	L
	0.00	1.00	0.85	1.00	-3.48	60.4	BF
	0.00	1.00	0.80	0.30	-3.47	—	L
	0.05	0.95	0.87	1.00	-3.47	60.4	BF
	0.05	0.95	0.84	0.00	-3.47	—	L
	0.30	0.70	1.00	1.00	-3.44	61.4	BF
	0.30	0.70	1.00	0.00	-3.42	—	L
TBI	0.00	1.00	0.79	1.00	15.895	273.9	BF
	0.00	1.00	0.81	1.00	15.905	—	L
	0.00	1.00	0.79	1.00	15.895	273.8	BF
	0.00	1.00	0.75	1.00	15.905	—	L
	0.05	0.95	0.82	1.00	15.895	274.0	BF
	0.05	0.95	0.78	1.00	15.915	—	L
	0.30	0.70	0.97	1.00	15.915	275.8	BF
	0.30	0.70	0.96	0.00	15.915	—	L
TBII	0.00	1.00	0.78	1.00	15.915	186.5	BF
	0.00	1.00	0.81	1.00	15.925	—	L
	0.00	1.00	0.78	1.00	15.915	186.5	BF
	0.00	1.00	0.75	1.00	15.915	—	L
	0.05	0.95	0.81	1.00	15.915	186.6	BF
	0.05	0.95	0.78	1.00	15.925	—	L

2. Cosmological model

Einstein equations for the Friedman-Robertson-Walker model with hydrodynamical energy-momentum tensor $T_{\mu\nu} = (\rho + p)u_\mu u_\nu - pg_{\mu\nu}$ read:

$$\left(\frac{\dot{a}}{a}\right)^2 = \frac{8\pi G\rho}{3} - \frac{k}{a^2(t)} \quad (1)$$

$$\frac{\ddot{a}(t)}{a} = -\frac{4\pi G}{3}(\rho + 3p) \quad (2)$$

Let us assume that matter content of the Universe consists of pressure-less gas with energy density ρ_m representing baryonic plus cold dark matter (CDM) and the Generalized Chaplygin Gas with the equation of state

$$p_{Ch} = -\frac{A}{\rho_{Ch}^\alpha} \quad (3)$$

representing the dark energy responsible for the acceleration of the Universe. If one further makes an assumption that these two components do not interact, then the energy conservation equation

$$\dot{\rho} + 3H(p + \rho) = 0 \quad (4)$$

where $H = \dot{a}/a$ is the Hubble function, can be integrated separately for matter and Chaplygin gas leading to well known result $\rho_m = \rho_{m,0}a^{-3}$ and (see also Bento, Bertolami & Sen 2002 or Carturan & Finelli 2002)

$$\rho_{Ch} = \left(A + \frac{B}{a^{3(1+\alpha)}}\right)^{\frac{1}{1+\alpha}} \quad (5)$$

The physical interpretation of, so far arbitrary, constants A and B is the following. Adopting usual convention that current value of the scale factor a_0 is equal to 1, one can see that $\rho_{Ch,0} = (A + B)^{\frac{1}{1+\alpha}}$ represents the current energy density of the Chaplygin gas. Calculating the adiabatic speed of sound squared for the Chaplygin gas

$$c_s^2 = \frac{\partial p_{Ch}}{\partial \rho_{Ch}} = \frac{\alpha A}{\rho^{1+\alpha}} = \frac{\alpha A}{A + \frac{B}{a^{3(1+\alpha)}}}$$

it is easy to confirm that the current value of c_s^2 is equal to $c_{s,0}^2 = \frac{\alpha A}{A+B}$. Hence the constants A and B can be expressed as combinations of quantities having well defined physical meaning.

Our further task will be to confront the Chaplygin gas model with SNIa data and for this purpose we have to calculate the luminosity distance in our model

$$d_L(z) = (1+z) \frac{c}{H_0 \sqrt{|\Omega_k|}} \mathcal{F} \left(H_0 \sqrt{|\Omega_k|} \int_0^z \frac{dz'}{H(z')} \right) \quad (6)$$

Table 1—Continued

sample	Ω_m	Ω_{Ch}	A_0	α	\mathcal{M}	χ^2	method
Silver	0.30	0.70	0.97	1.00	15.925	188.4	BF
	0.30	0.70	0.96	0.00	15.935	—	L
	0.00	1.00	0.82	1.00	15.945	229.4	BF
	0.00	1.00	0.84	1.00	15.945	—	L
	0.00	1.00	0.82	1.00	15.945	229.4	BF
	0.00	1.00	0.79	1.00	15.955	—	L
	0.05	0.95	0.85	1.00	15.945	229.6	BF
	0.05	0.95	0.81	1.00	15.955	—	L
	0.30	0.70	0.99	1.00	15.965	232.3	BF
	0.30	0.70	0.99	0.00	15.965	—	L
Gold	0.00	1.00	0.81	1.00	15.945	173.7	BF
	0.00	1.00	0.83	1.00	15.955	—	L
	0.00	1.00	0.81	1.00	15.945	173.7	BF
	0.00	1.00	0.77	1.00	15.955	—	L
	0.05	0.95	0.84	1.00	15.945	173.8	BF
	0.05	0.95	0.80	1.00	15.955	—	L
	0.30	0.70	0.99	1.00	15.965	175.6	BF
	0.30	0.70	0.99	0.00	15.965	—	L

Table 2: Generalized Chaplygin Gas model parameter values obtained from the marginal probability density functions calculated on Perlmutter, Knop, Tonry/Barris and Riess samples with Ω_m prior relaxed.

sample	Ω_m	Ω_{Ch}	A_0	α
A	$0.17^{+0.08}_{-0.17}$	$0.83^{+0.17}_{-0.08}$	$0.83^{+0.14}_{-0.09}$	$-0.0^{+0.67}$
C	$0.15^{+0.08}_{-0.15}$	$0.85^{+0.15}_{-0.08}$	$0.86^{+0.13}_{-0.10}$	$0.0^{+0.66}$
K6	$0.10^{+0.11}_{-0.10}$	$0.90^{+0.10}_{-0.11}$	$0.88^{+0.12}_{-0.08}$	$-0.0^{+0.66}$
K3	$0.11^{+0.07}_{-0.11}$	$0.89^{+0.11}_{-0.07}$	$0.88^{+0.11}_{-0.05}$	$0.0^{+0.66}$
TBI	$0.00^{+0.21}$	$1.00_{-0.21}$	$0.81^{+0.12}_{-0.07}$	$1.0_{-0.60}$
TBII	$0.00^{+0.21}$	$1.00_{-0.21}$	$0.81^{+0.12}_{-0.07}$	$1.0_{-0.62}$
Silver	$0.00^{+0.18}$	$1.00_{-0.18}$	$0.84^{+0.09}_{-0.06}$	$1.0_{-0.59}$
Gold	$0.00^{+0.20}$	$1.00_{-0.20}$	$0.83^{+0.11}_{-0.07}$	$1.0_{-0.64}$

Table 3: Generalized Chaplygin Gas model parameter values obtained from the marginal probability density functions calculated on Perlmutter, Knop, Tonry/Barris and Riess samples. The analysis was done with fixed $\Omega_m = 0.0$, $\Omega_m = 0.05$ and $\Omega_m = 0.3$.

sample	Ω_m	Ω_{Ch}	A_0	α
A	0.00	1.00	$0.73^{+0.08}_{-0.10}$	$1.0_{-0.63}$
	0.05	0.95	$0.76^{+0.08}_{-0.09}$	$1.0_{-0.66}$
	0.30	0.70	$0.96^{+0.04}_{-0.09}$	$0.0^{+0.65}$
C	0.00	1.00	$0.76^{+0.08}_{-0.10}$	$0.49^{+0.36}_{-0.35}$
	0.05	0.95	$0.79^{+0.08}_{-0.11}$	$0.41^{+0.27}_{-0.41}$
	0.30	0.70	$0.99^{+0.01}_{-0.11}$	$0.0^{+0.64}$
K6	0.00	1.00	$0.78^{+0.07}_{-0.09}$	$0.71^{+0.29}_{-0.40}$
	0.05	0.95	$0.81^{+0.08}_{-0.09}$	$0.06^{+0.61}_{-0.06}$
	0.30	0.70	$1.00_{-0.10}$	$0.0^{+0.64}$
K3	0.00	1.00	$0.80^{+0.06}_{-0.06}$	$0.30^{+0.39}_{-0.30}$
	0.05	0.95	$0.84^{+0.05}_{-0.07}$	$0.0^{+0.67}$
	0.30	0.70	$1.00_{-0.06}$	$0.0^{+0.63}$
TBI	0.00	1.00	$0.75^{+0.04}_{-0.05}$	$1.0_{-0.54}$
	0.05	0.95	$0.78^{+0.04}_{-0.06}$	$1.0_{-0.55}$
	0.30	0.70	$0.96^{+0.04}_{-0.04}$	$0.0^{+0.67}$
TBII	0.00	1.00	$0.75^{+0.04}_{-0.06}$	$1.0_{-0.54}$
	0.05	0.95	$0.78^{+0.04}_{-0.06}$	$1.0_{-0.54}$
	0.30	0.70	$0.96^{+0.04}_{-0.04}$	$0.0^{+0.67}$
Silver	0.00	1.00	$0.79^{+0.03}_{-0.05}$	$1.0_{-0.52}$
	0.05	0.95	$0.81^{+0.04}_{-0.04}$	$1.0_{-0.54}$
	0.30	0.70	$0.99^{+0.01}_{-0.03}$	$0.0^{+0.64}$
Gold	0.00	1.00	$0.77^{+0.04}_{-0.05}$	$1.0_{-0.58}$
	0.05	0.95	$0.80^{+0.04}_{-0.05}$	$1.0_{-0.59}$
	0.30	0.70	$0.99^{+0.01}_{-0.04}$	$0.0^{+0.64}$

Table 4: Results of statistical analysis of Generalized Chaplygin Gas models with flat prior relaxed and with marginalization over \mathcal{M} performed on Knop Samples K3 as a minimum χ^2 best-fit(denoted BF) and with the maximum likelihood method (denoted L). First two rows refer to no prior on Ω_m . The same analysis was repeated with fixed $\Omega_m = 0.0$, $\Omega_m = 0.05$ and $\Omega_m = 0.3$.

sample	Ω_k	Ω_m	Ω_{Ch}	A_0	α	\mathcal{M}	χ^2	method
K3	-0.19	0.00	1.19	0.82	1.00	-3.48	60.3	BF
	-0.60	0.00	1.26	0.89	0.00	-3.46	—	L
	-0.25	0.00	1.25	0.82	1.00	-3.49	60.3	BF
	0.10	0.00	0.90	0.76	0.00	-3.46	—	L
	-0.28	0.05	1.23	0.84	1.00	-3.49	60.3	BF
	0.05	0.05	0.90	0.78	0.00	-3.47	—	L
	-0.48	0.30	1.18	0.93	0.97	-3.49	60.3	BF
	-0.35	0.30	1.05	0.88	0.00	-3.47	—	L
Gold	-0.12	0.00	1.12	0.80	0.99	15.945	173.4	BF
	-0.32	0.00	1.06	0.82	0.00	15.945	—	L
	-0.13	0.00	1.13	0.81	1.00	15.935	173.4	BF
	-0.19	0.00	1.19	0.76	0.85	15.945	—	L
	-0.17	0.05	1.12	0.83	1.00	15.935	173.4	BF
	-0.20	0.05	1.15	0.78	0.54	15.945	—	L
	-0.31	0.30	1.01	0.94	1.00	15.955	173.6	BF
	-0.30	0.30	1.00	0.91	0.00	15.945	—	L

Table 5: Results of statistical analysis of Generalized Chaplygin Gas models with flat prior relaxed and with marginalization over \mathcal{M} performed on Knop Samples K3. Model parameter values are obtained from the marginal probability density functions. First row refer to no prior on Ω_m . The same analysis was repeated with fixed $\Omega_m = 0.0$, $\Omega_m = 0.05$ and $\Omega_m = 0.3$.

sample	Ω_k	Ω_m	Ω_{Ch}	A_0	α
K3	$-0.60^{+0.38}_{-0.38}$	$0.00^{+0.29}$	$1.26^{+0.25}_{-0.39}$	$0.89^{+0.11}_{-0.07}$	$0.0^{+0.64}$
	$0.10^{+0.37}_{-0.60}$	0.00	$0.90^{+0.59}_{-0.37}$	$0.76^{+0.10}_{-0.07}$	$0.0^{+0.66}$
	$0.05^{+0.31}_{-0.58}$	0.05	$0.90^{+0.58}_{-0.31}$	$0.78^{+0.10}_{-0.06}$	$0.0^{+0.66}$
	$-0.35^{+0.17}_{-0.40}$	0.30	$1.05^{+0.41}_{-0.17}$	$0.88^{+0.09}_{-0.05}$	$0.0^{+0.63}$
Gold	$-0.32^{+0.25}_{-0.25}$	$0.00^{+0.28}$	$1.06^{+0.24}_{-0.22}$	$0.82^{+0.13}_{-0.05}$	$0.0^{+0.64}$
	$-0.19^{+0.29}_{-0.28}$	0.00	$1.19^{+0.28}_{-0.29}$	$0.76^{+0.03}_{-0.05}$	$0.85^{+0.15}_{-0.52}$
	$-0.20^{+0.28}_{-0.29}$	0.05	$1.15^{+0.29}_{-0.28}$	$0.78^{+0.05}_{-0.06}$	$0.54^{+0.36}_{-0.32}$
	$-0.30^{+0.21}_{-0.23}$	0.30	$1.00^{+0.23}_{-0.21}$	$0.91^{+0.04}_{-0.05}$	$0.00^{+0.60}$

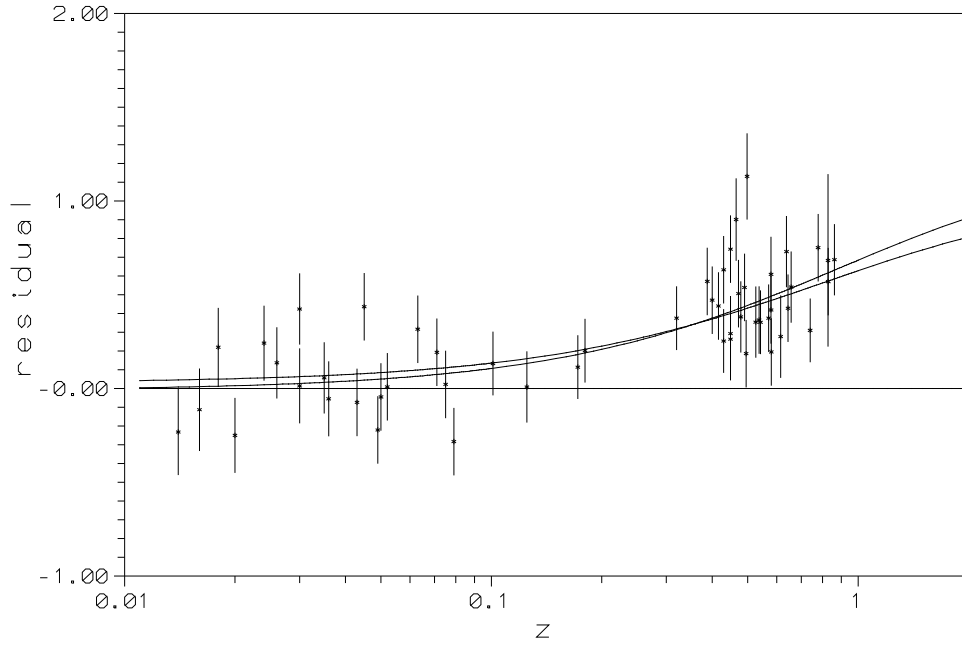


Fig. 1.— Residuals (in mag) between the Einstein-de Sitter model (zero line), the Λ CDM model (upper curve) and the best-fitted Generalized Chaplygin Gas model with $\Omega_m = 0.3, \Omega_{Ch} = 0.7$ (middle curve), sample K3.

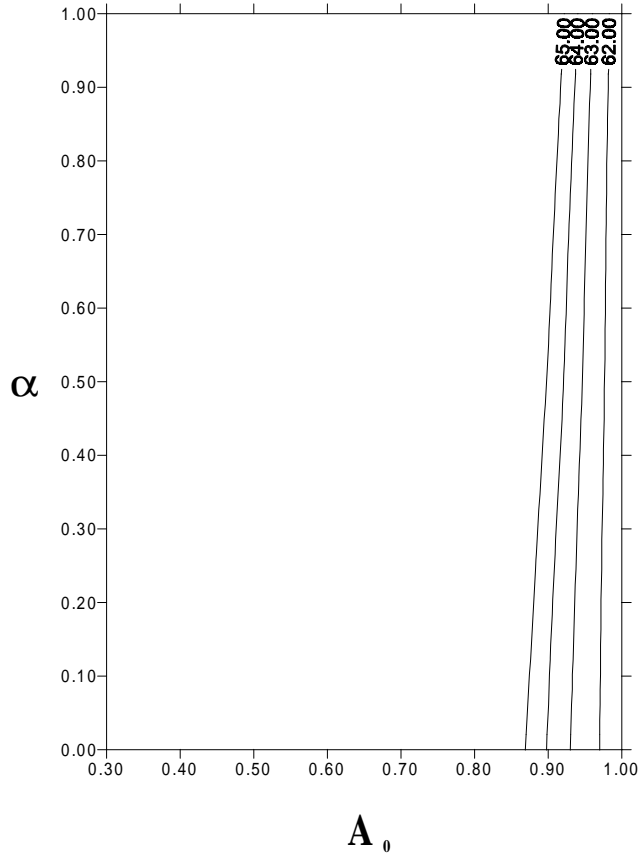


Fig. 2.— Levels of constant χ^2 on the plane (A_0, α) for Generalized Chaplygin Gas model with $\Omega_m = 0.3, \Omega_{Ch} = 0.7$, sample K3, marginalized over \mathcal{M} . The figure shows preferred values of A_0 and α .

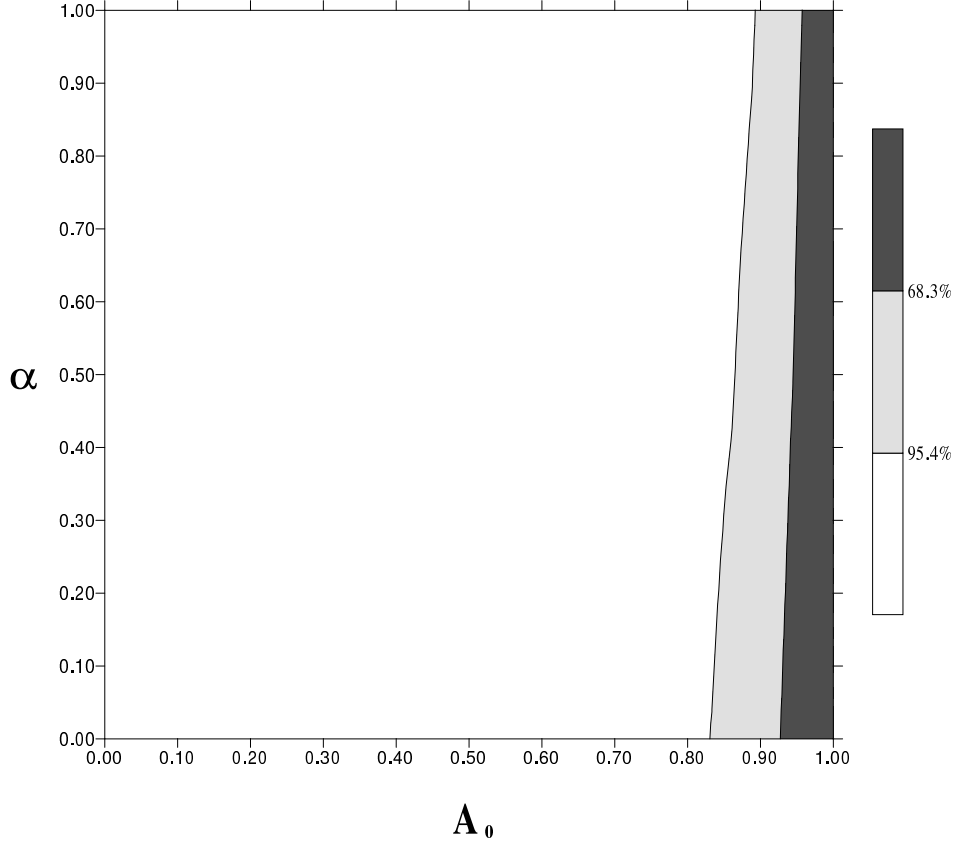


Fig. 3.— Confidence levels on the plane (A_0, α) for Generalized Chaplygin Gas model with $\Omega_m = 0.3, \Omega_{Ch} = 0.7$, sample K3, marginalized over \mathcal{M} . The figure shows the ellipses of preferred values of A_0 and α .

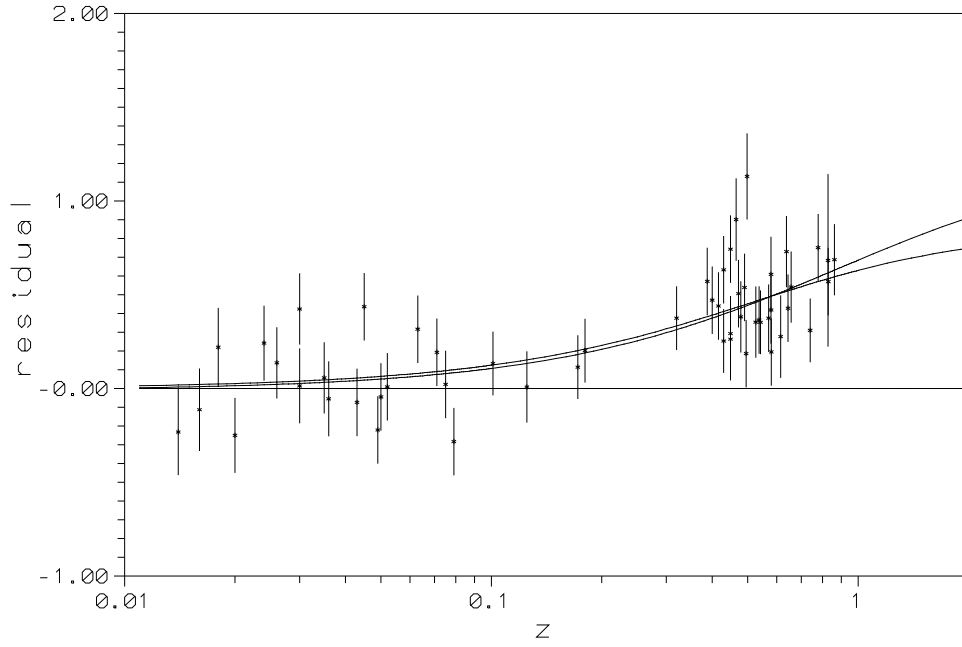


Fig. 4.— Residuals (in mag) between the Einstein-de Sitter model (zero line), the flat Λ CDM model (upper curve) and the best-fitted Generalized Chaplygin Gas model with $\Omega_m = 0.05, \Omega_{Ch} = 0.95$ (middle curve), sample K3.

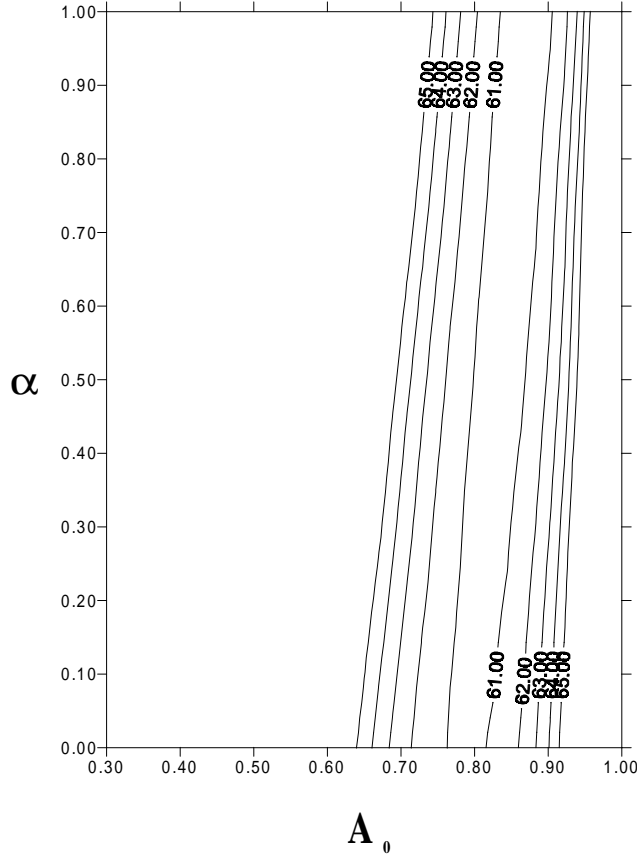


Fig. 5.— Levels of constant χ^2 on the plane (A_0, α) for Generalized Chaplygin Gas model with $\Omega_m = 0.05, \Omega_{Ch} = 0.95$, sample K3, marginalized over \mathcal{M} . The figure shows preferred values of A_0 and α .

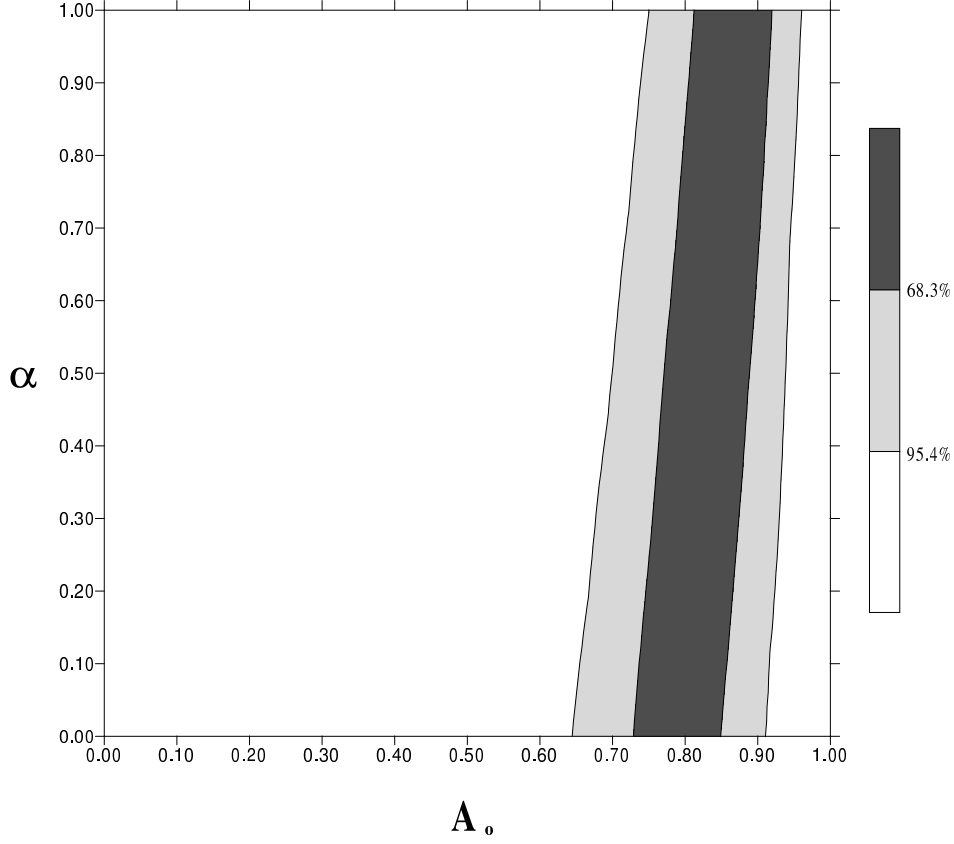


Fig. 6.— Confidence levels on the plane (A_0, α) for Generalized Chaplygin Gas model with $\Omega_m = 0.05, \Omega_{Ch} = 0.95$, sample K3, marginalized over \mathcal{M} . The figure shows the ellipses of preferred values of A_0 and α .

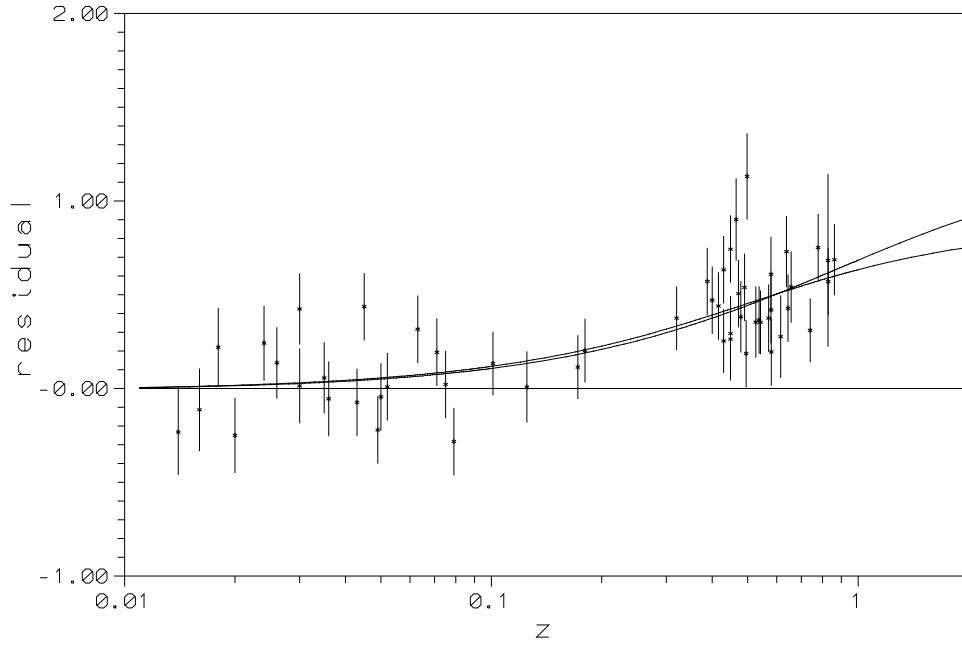


Fig. 7.— Residuals (in mag) between the Einstein-de Sitter model (zero line), the flat Λ CDM model (upper curve) and the best-fitted Generalized Chaplygin Gas model with $\Omega_m = 0, \Omega_{Ch} = 1$ (middle curve), sample K3.

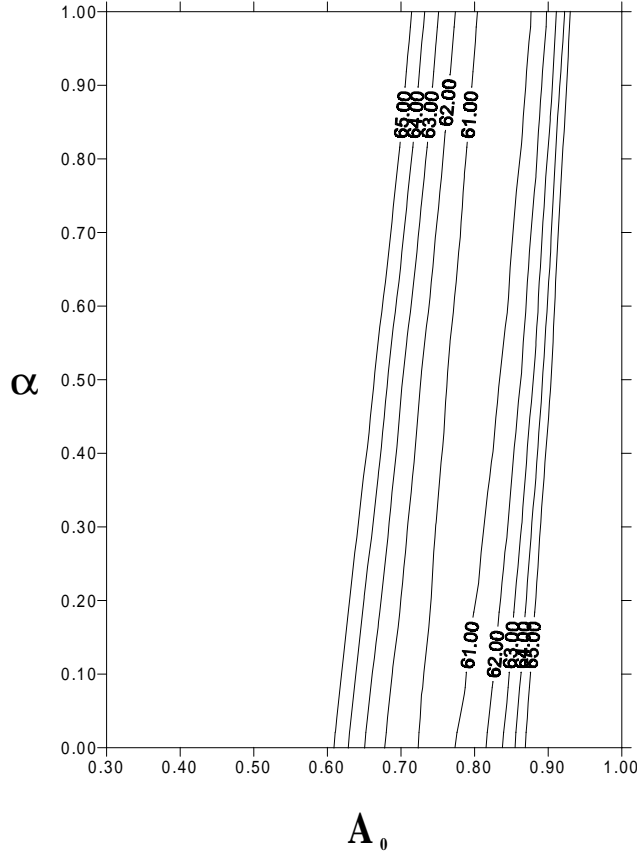


Fig. 8.— Levels of constant χ^2 on the plane (A_0, α) for Generalized Chaplygin Gas model with $\Omega_m = 0, \Omega_{Ch} = 1$, sample K3, marginalized over \mathcal{M} . The figure shows preferred values of A_0 and α .

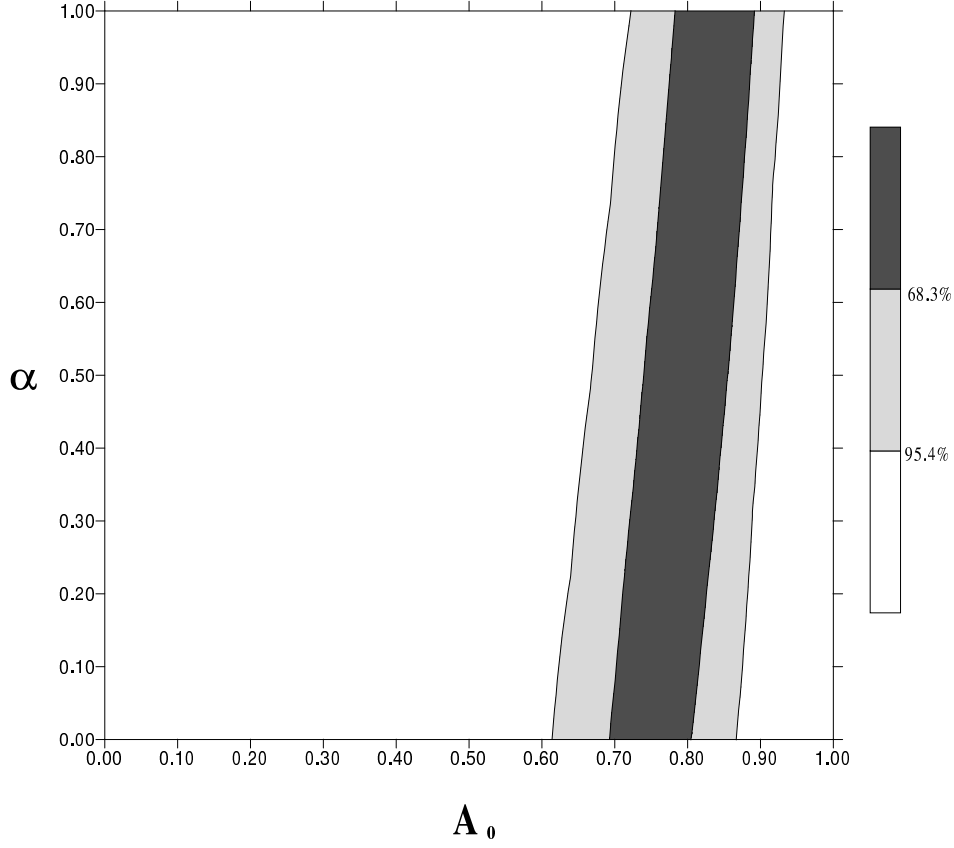


Fig. 9.— Confidence levels on the plane (A_0, α) for Generalized Chaplygin Gas model with $\Omega_m = 0, \Omega_{Ch} = 1$, sample K3, marginalized over \mathcal{M} . The figure shows the ellipses of preferred values of A_0 and α .

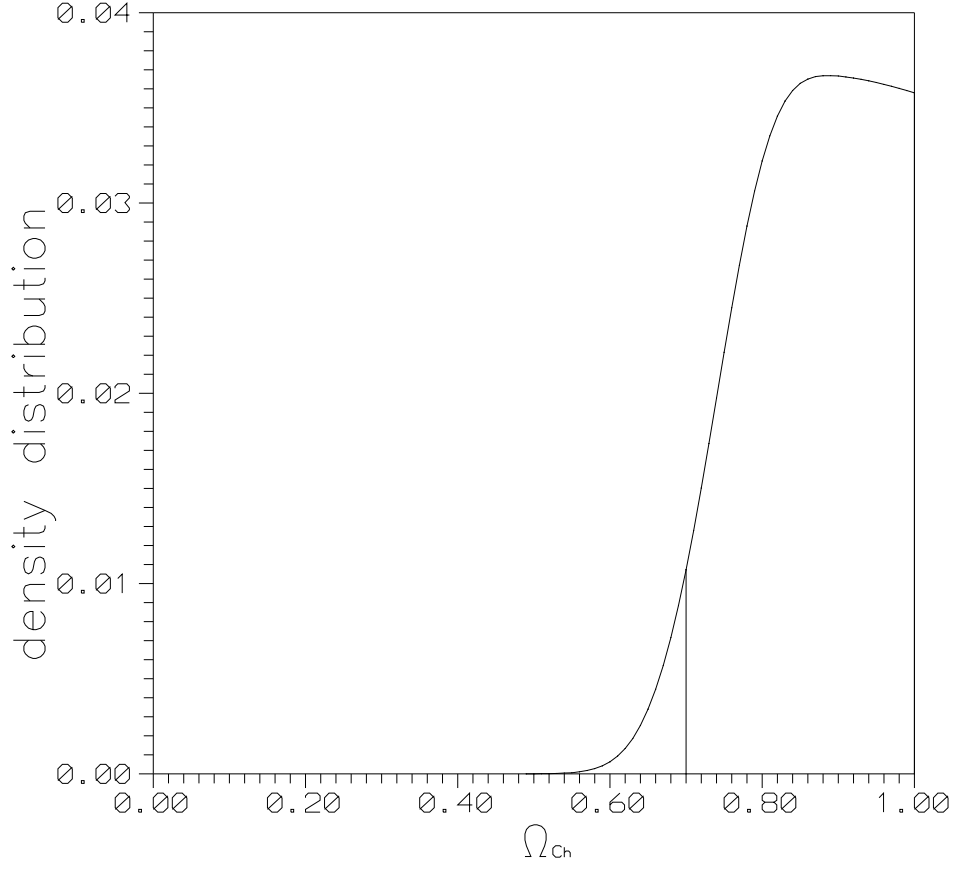


Fig. 10.— The density distribution (one dimensional PDF) for Ω_{Ch} obtained from sample K3 by marginalization over remaining parameters of the model. We obtain the limit $\Omega_{Ch} > 0.70$ at the confidence level 95.4%.

where $\Omega_k = -\frac{k}{H_0^2}$ and

$$\mathcal{F}(x) = \sinh(x) \quad \text{for} \quad k < 0 \quad (7)$$

$$\mathcal{F}(x) = x \quad \text{for} \quad k = 0 \quad (8)$$

$$\mathcal{F}(x) = \sin(x) \quad \text{for} \quad k > 0 \quad (9)$$

The Friedman equation (1) can be rearranged to the form giving explicitly the Hubble function $H(z) = \dot{a}/a$

$$H(z)^2 = H_0^2 \left[\Omega_m(1+z)^3 + \Omega_{Ch} \left(A_0 + (1-A_0)(1+z)^{3(1+\alpha)} \right)^{\frac{1}{1+\alpha}} + \Omega_k(1+z)^2 \right] \quad (10)$$

where the quantities Ω_i , $i = m, Ch, k$ represent fractions of critical density currently contained in energy densities of respective components and $\Omega_m + \Omega_{Ch} + \Omega_k = 1$. For the transparency of further formulae we have also denoted $A_0 = A/(A+B)$.

Finally the luminosity distance reads:

$$d_L(z) = (1+z) \frac{c}{H_0} \frac{1}{\sqrt{|\Omega_k|}} \mathcal{F} \left(\sqrt{|\Omega_k|} \int_0^z \frac{dz'}{\sqrt{\Omega_m(1+z)^3 + \Omega_{Ch} \left(A_0 + (1-A_0)(1+z)^{3(1+\alpha)} \right)^{\frac{1}{1+\alpha}} + \Omega_k(1+z)^2}} \right) \quad (11)$$

The formula (11) is the most general one in the framework of Friedman-Robertson-Walker cosmology with Generalized Chaplygin Gas. Please note, that this model propose a unified macroscopic (phenomenological) description of both dark energy and dark matter.

Further in this paper we will mostly use its version restricted to flat model $k = 0$ (the exception will be when we relax flat prior) since the evidence for this case is very strong in the light of current CMBR data. Therefore while talking about model testing we actually mean the estimation of α and A_0 parameters for the best fitted flat FRW cosmological model filled with Generalized Chaplygin Gas.

To proceed with fitting the SNIa data we need the magnitude-redshift relation

$$m(z, \mathcal{M}, \Omega_m, \Omega_{Ch}; A_0, \alpha) = \mathcal{M} + 5 \log_{10} D_L(z, \Omega_m, \Omega_{Ch}; A_0, \alpha) \quad (12)$$

where:

$$D_L(z, \Omega_m, \Omega_{Ch}; A_0, \alpha) = H_0 d_L(z, H_0, \Omega_m, \Omega_{Ch}; A_0, \alpha)$$

is the luminosity distance with H_0 factored out so that marginalization over the intercept

$$\mathcal{M} = M - 5 \log_{10} H_0 + 25 \quad (13)$$

leads actually to joint marginalization over H_0 and M (M being the absolute magnitude of SNIa).

Then we can obtain the best fitted model minimalizing the χ^2 function

$$\chi^2 = \sum_i \frac{(m_i^{Ch} - m_i^{obs})^2}{\sigma_i^2}$$

where the sum is over the SNIa sample and σ_i denote the (full) statistical error of magnitude determination. This is illustrated by figures (Fig.1 - Fig.9) of residuals (with respect to Einstein-de Sitter model) and χ^2 levels in the (A_0, α) plane. One of the advantages of residual plots is that the intercept of the $m - z$ curve gets cancelled. The assumption that the intercept is the same for different cosmological models is legitimate since \mathcal{M} is actually determined from the low-redshift part of the Hubble diagram which should be linear in all realistic cosmologies. From the full Perlmutter's sample (see below) we have obtained $\mathcal{M} = -3.39$ which is in a very good agreement with the values reported in the literature (Perlmutter et al. 1999, Riess et al. 1999). For other samples see discussion below.

The best-fit values alone are not relevant if not supplemented with the confidence levels for the parameters. Therefore, we performed the estimation of model parameters using the minimization procedure, based on the likelihood function. We assumed that supernovae measurements came with uncorrelated Gaussian errors and in this case the likelihood function \mathcal{L} could be determined from chi-square statistic $\mathcal{L} \propto \exp(-\chi^2/2)$ (Perlmutter et al. 1999, Riess et al. 1999).

Therefore we supplement our analysis with confidence intervals in the (A_0, α) plane by calculating the marginal probability density functions

$$\mathcal{P}(A_0, \alpha) \propto \int \exp(-\chi^2(\Omega_m, \Omega_{Ch}, A_0, \alpha, \mathcal{M})/2) d\mathcal{M}$$

with Ω_m, Ω_{Ch} fixed ($\Omega_m = 0.0, 0.05, 0.3$) and

$$\mathcal{P}(A_0, \alpha) \propto \int \exp(-\chi^2(\Omega_m, \Omega_{Ch}, A_0, \alpha, \mathcal{M})/2) d\Omega_m$$

with \mathcal{M} fixed ($\mathcal{M} = -3.39$) respectively (proportionality sign means equal up to the normalization constant). In order to complete the picture we have also derived one-dimensional probability distribution functions for Ω_{Ch} obtained from joint marginalization over α and A_0 . The maximum value of such PDF informs us about the most probable value of Ω_{Ch} (supported by supernovae data) within the full class of Generalized Chaplygin Gas models.

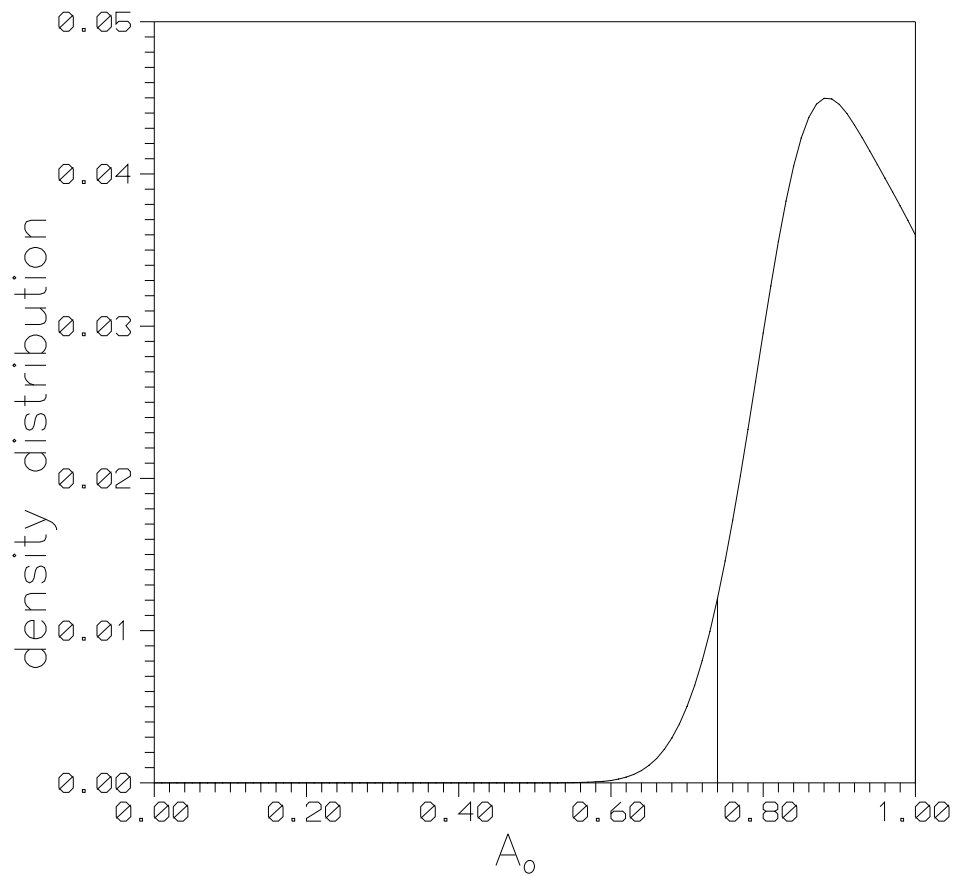


Fig. 11.— The density distribution (one dimensional PDF) for A_0 obtained from sample K3 by marginalization over remaining parameters of the model. We obtain the limit $A_0 > 0.74$ at the confidence level 95.4%.

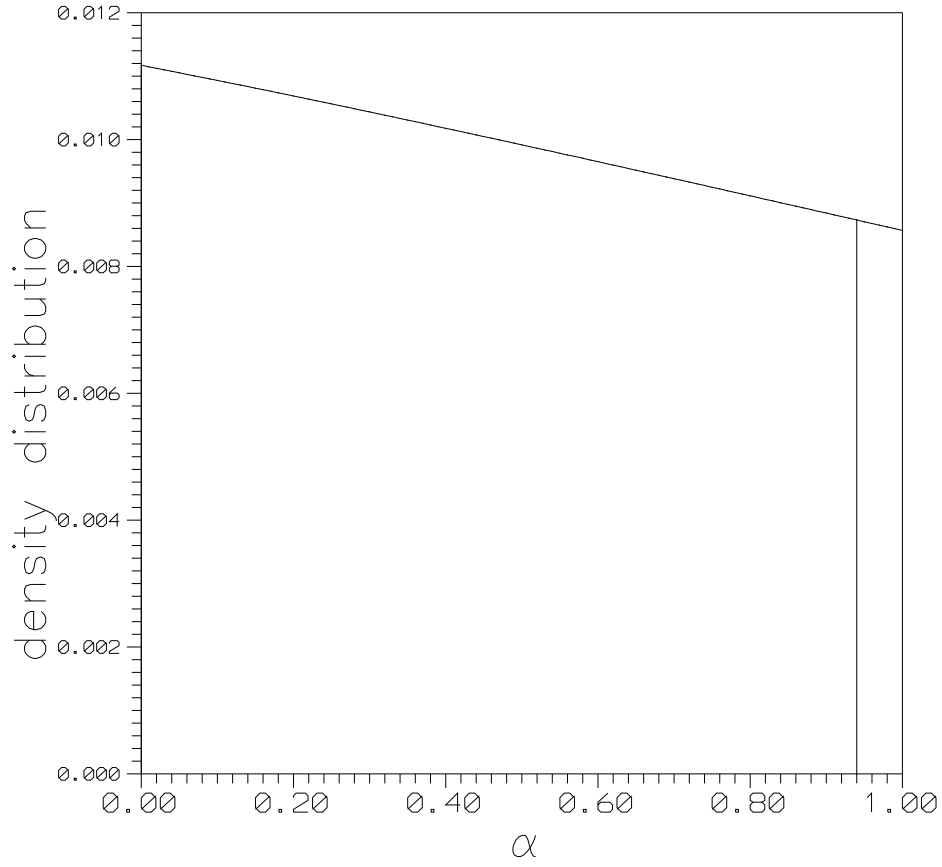


Fig. 12.— The density distribution (one dimensional PDF) for α obtained from sample K3 by marginalization over remaining parameters of the model. We obtain the limit $\alpha < 0.94$ at the confidence level 95.4% .

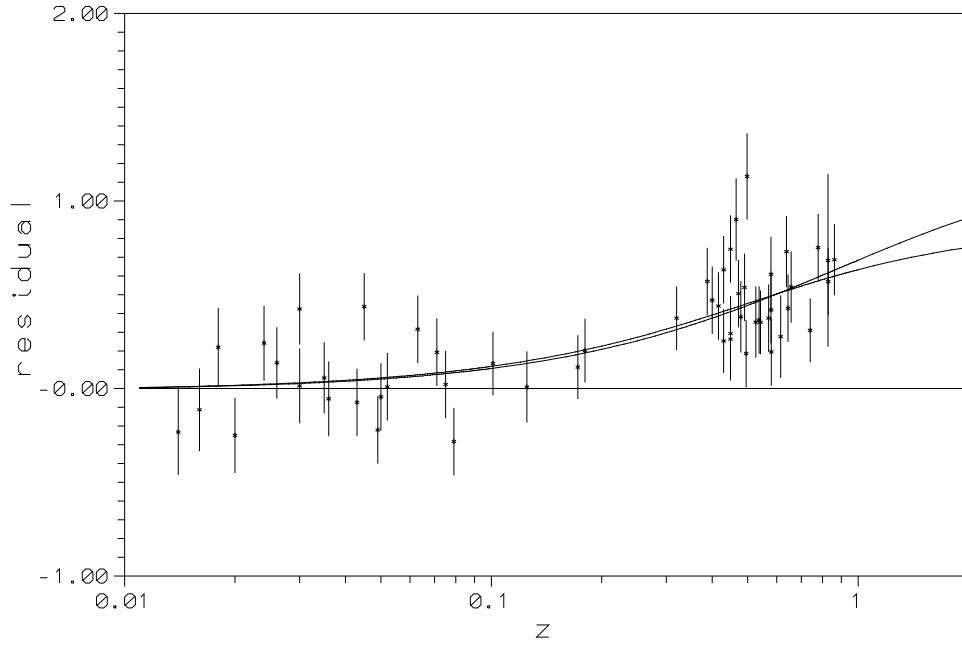


Fig. 13.— Residuals (in mag) between the Einstein-de Sitter model (zero line), the flat Λ CDM model (upper curve) and the best-fitted Generalized Chaplygin Gas model (without any prior assumptions on Ω_m) (middle curve), sample K3.

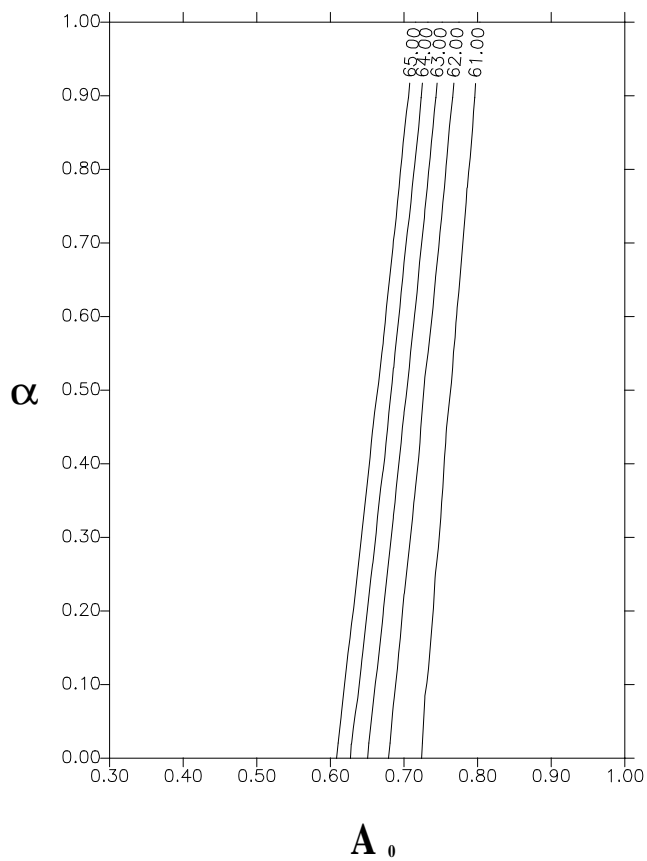


Fig. 14.— Levels of constant χ^2 on the plane (A_0, α) for Generalized Chaplygin Gas model, sample K3, marginalized over \mathcal{M} , and Ω_m . The figure shows preferred values of A_0 and α .

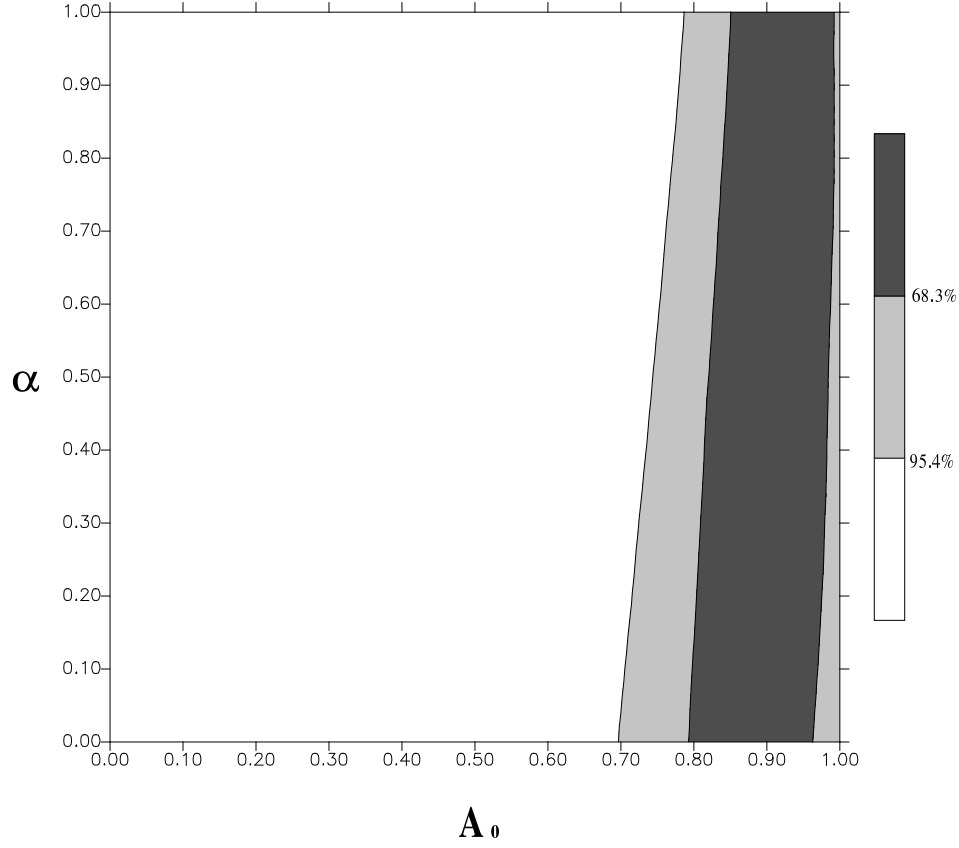


Fig. 15.— Confidence levels on the plane (A_0, α) for Generalized Chaplygin Gas model, sample K3, marginalized over \mathcal{M} , and Ω_m . The figure shows the ellipses of preferred values of A_0 and α .

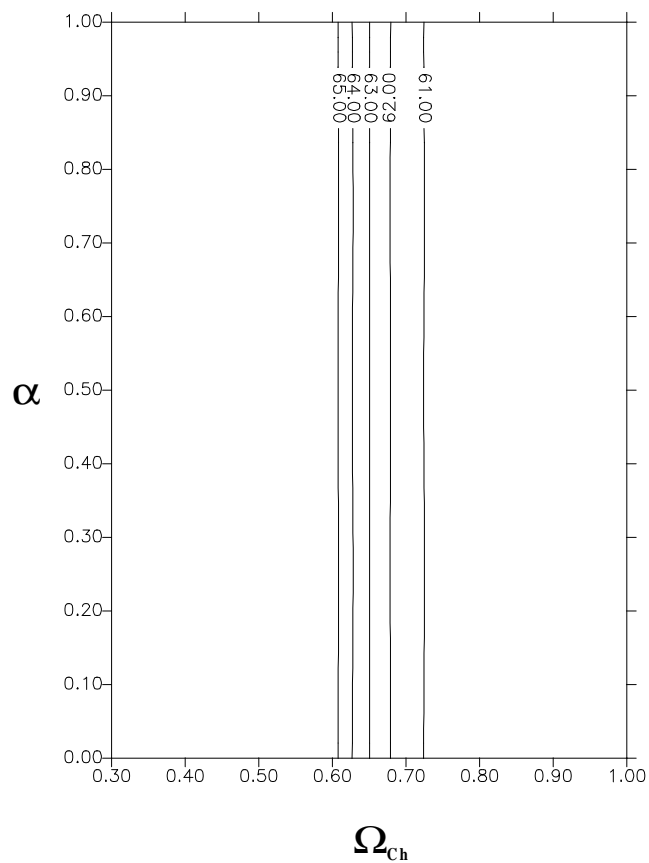


Fig. 16.— Levels of constant χ^2 on the plane (Ω_m, α) for Generalized Chaplygin Gas model, sample K3, marginalized over \mathcal{M} , and A_0 . The figure shows preferred values of Ω_m , and α .

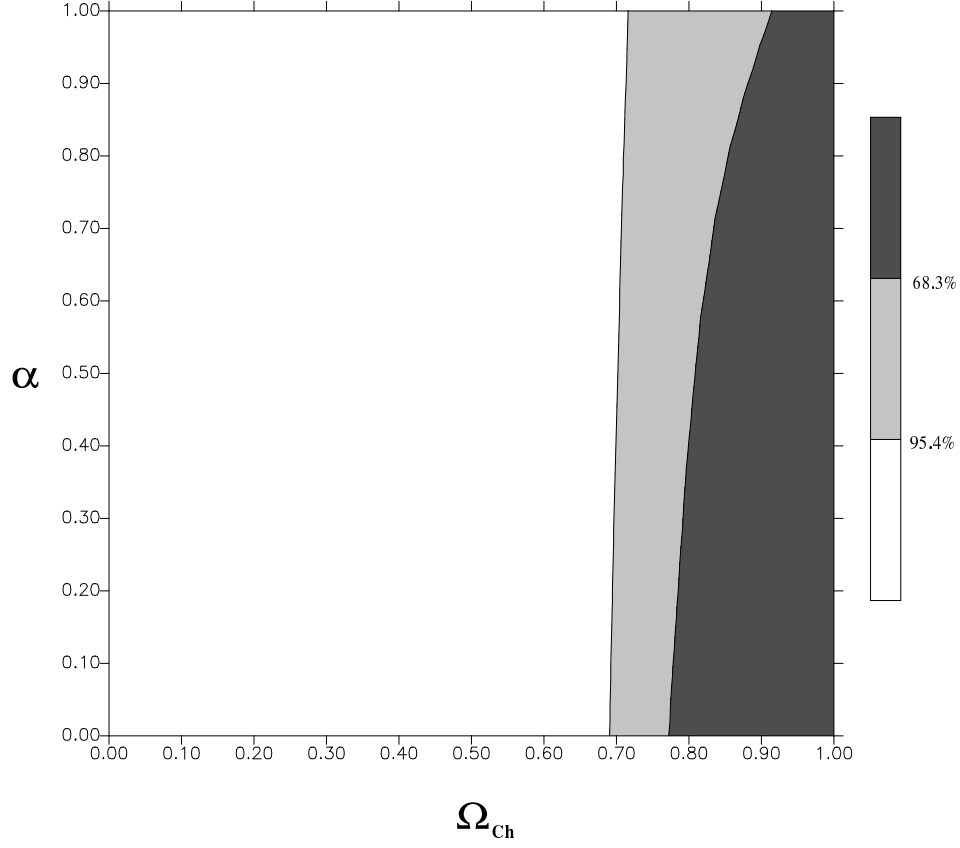


Fig. 17.— Confidence levels on the plane (Ω_m, α) for Generalized Chaplygin Gas model, sample K3, marginalized over \mathcal{M} , and A_0 . The figure shows the ellipses of preferred values of Ω_m , and α .

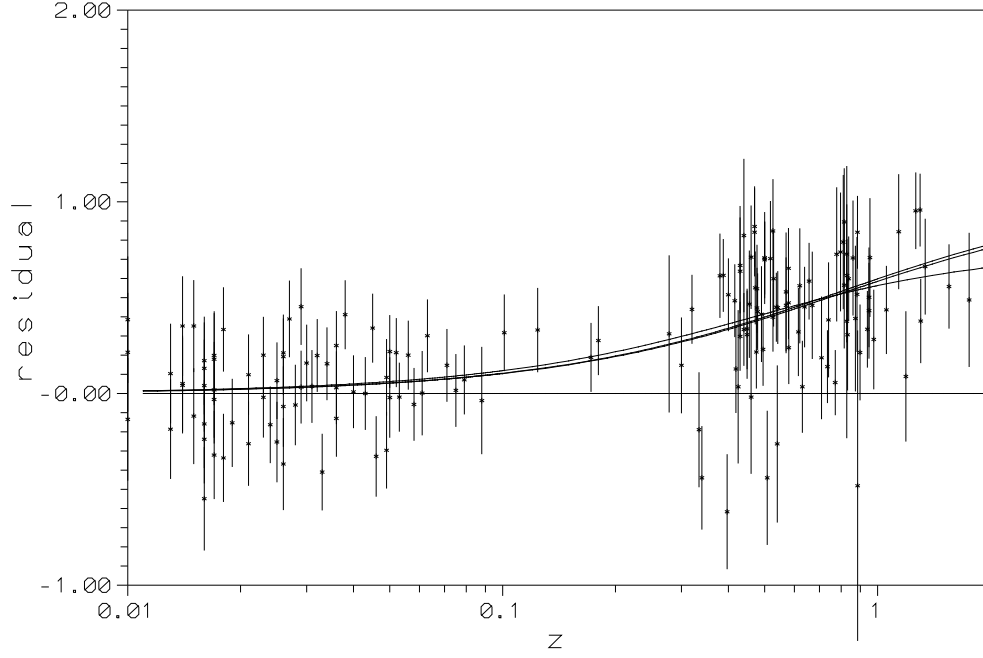


Fig. 18.— Residuals (in mag) between the Einstein-de Sitter model (zero line), flat Λ CDM model (two upper curves: for SNIa with $z < 1$ — curve located higher and for all supernovae Ia belonging to the sample — curve located lower) and the best-fitted Generalized Chaplygin Gas model (without any prior assumptions on Ω_m) (middle curve), GOLD sample.

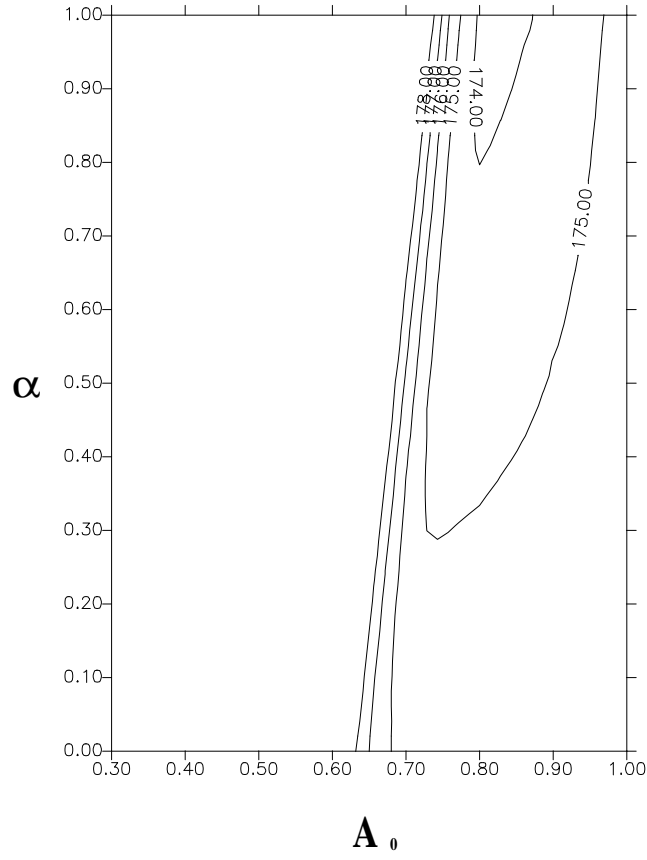


Fig. 19.— Levels of constant χ^2 on the plane (A_0, α) for Generalized Chaplygin Gas model, Gold sample, marginalized over \mathcal{M} , and Ω_m . The figure shows preferred values of A_0 and α .

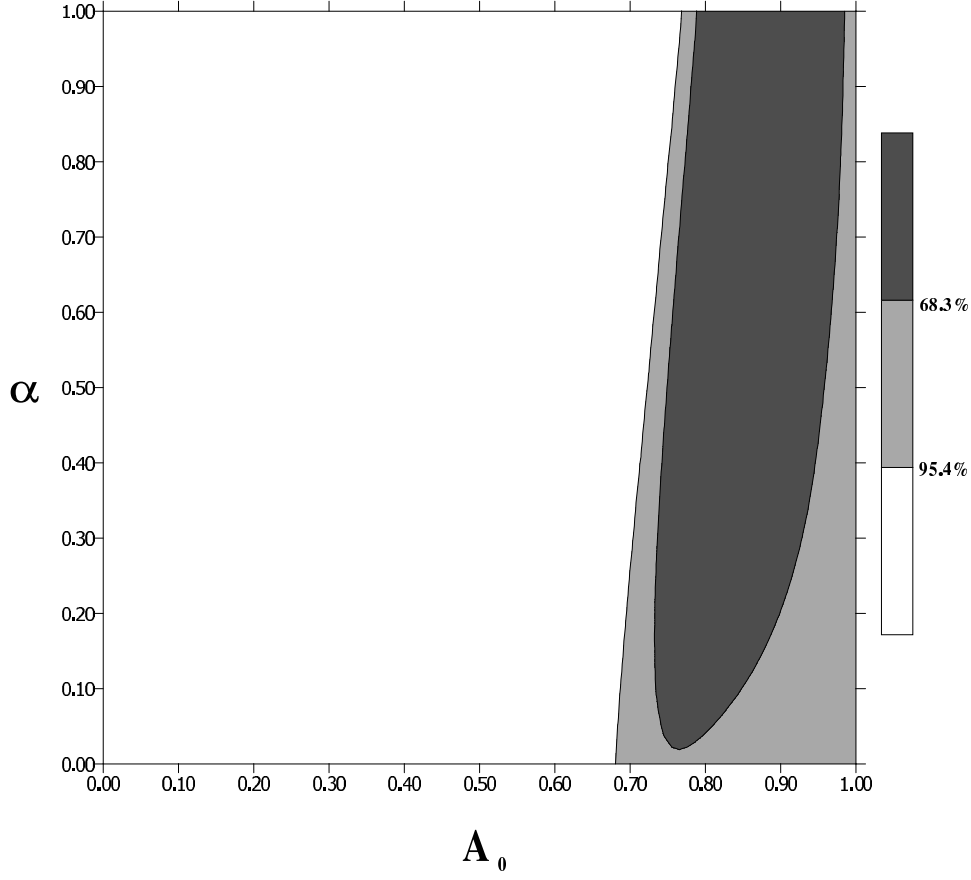


Fig. 20.— Confidence levels on the plane (A_0, α) for Generalized Chaplygin Gas model, Gold sample, marginalized over \mathcal{M} , and Ω_m . The figure shows the ellipses of preferred values of A_0 and α .

3. Fits to A_0 and α parameters

3.1. Samples used

Supernovae surveys (published data) have already five years long history. Beginning with first published samples other data sets have been produced either by correcting original samples for systematics or by supplementing them with new supernovae (or both). It is not our intention here to suggest a distinguished role to any one of these data sets. Therefore, in our analysis we decided to use a collection of samples from all existing supernovae data.

Latest data was compiled by Riess et al. (2004). However, for comparison and illustration we analyse three other main samples of supernovae. Such investigation seems to be useful because it is pointed out in the literature that result of the analysis with different SNIa sample give often different results (see for example Godłowski Szydlowski & Krawiec 2003, Choudhury & Padmanabhan 2004).

Samples from the original Perlmutter et al. (1999) data chosen for the analysis comprise the full sample reported by Perlmutter (sample A) and a sub-sample after excluding two outliers differing the most from the average lightcurve and two outliers claimed to be likely reddened (sample C). Although the outliers often suggest statistical inhomogeneity of the data (and some hints suggesting the necessity of removing them from sample A exist) there is always a danger that removal of outliers is to some extent subjective. Therefore we retained the full sample A in our analysis. The Perlmutter data were gathered some years ago, hence one should also refer to more recent supernovae data as well.

Recently Knop et al. (2003) have reexamined the Perlmutter's data with host-galaxy extinction correctly assessed. From the Perlmutter's sample they chose only these supernovae which were spectroscopically safely identified as type Ia and had reasonable color measurements. They also included eleven new high redshift supernovae and a well known sample with low redshift supernovae. In Knop et al. (2003) a few subsamples have been distinguished. We considered two of them. The first is a subset of 58 supernovae with corrected extinction (Knop subsample 6; hereafter K6) and the second is that of 54 low extinction supernovae (Knop subsample 3; hereafter K3). Samples C and K3 are similarly constructed as containing only low extinction supernovae. The advantage of the Knop sample is that Knop's discussion of extinction correction was very careful and as a result his sample has extinction correctly applied.

Another sample was recently presented by Tonry et al. (2003) who collected a large number of supernovae data published by different authors and added eight new high redshift SN Ia. This sample of 230 SN Ia was re-calibrated with a consistent zero point. Wherever

possible the extinction estimates and distance fitting were recalculated. Unfortunately, one was not able to do so for the full sample (for details see Table 8 in Tonry et al. (2003)). This sample was further improved by Barris et al. (2003) who added 23 high redshift supernovae including 15 at $z \geq 0.7$ thus doubling the published record of objects at these redshifts. Despite of the above mentioned problems, the analysis of our model using this sample of supernovae could be interesting. Hence for comparison, we decided to repeat our analysis with the Tonry/Barris sample.

We decided to analyze two Tonry/Barris subsamples. First, we considered the full Tonry/Barris sample of 253 SNe Ia (hereafter sample TBI). The sample contains 218 SNe Ia with low extinction. Because Tonry’s sample has a lot of outliers especially at low redshifts, we decided to analyze the sample where all low redshift ($z < 0.01$) supernovae were excluded. In the sample of 193 supernovae all SN Ia with low redshift and high extinction were removed (hereafter sample TBII).

Tonry et al. (2003) and Barris et al. (2003) presented the data of redshifts and luminosity distances for their supernovae sample. Therefore, Eqs. (12) and (13) should be modified appropriately (Williams et al. 2003):

$$m - M = 5 \log_{10}(D_L)_{\text{Tonry}} - 5 \log_{10} 65 + 25 \quad (14)$$

and

$$\mathcal{M} = -5 \log_{10} H_0 + 25. \quad (15)$$

For the Hubble constant $H_0 = 65 \text{ km s}^{-1} \text{ Mpc}^{-1}$ one gets $\mathcal{M} = 15.935$.

Recently Riess et al. (2004) significantly improved the former Riess sample. They discovered 16 new type Ia Supernovae. It should be noted that 6 of these objects have $z > 1.25$ (out of total number of 7 object with so high redshifts). Moreover, they compiled a set of previously observed SNIa relying on large, published samples, whenever possible, to reduce systematic errors from differences in calibrations. With this enriched sample it became possible to test our prediction that distant supernovae in GCG cosmology should be brighter than in Λ CDM model (see discussion below). This is the reason why we repeated our analysis with new Riess sample.

The full Riess sample contains 186 SNIa (“Silver” sample). On the base of quality of the spectroscopic and photometric record for individual Supernovae, they also selected more restricted “Gold” sample of 157 Supernovae. We have separately analyzed Λ CDM model for supernovae with $z < 1$ and for all SNIa belonging to the Gold sample.

3.2. Cosmological models tested

On these samples we have tested Generalized Chaplygin gas cosmology in three different classes of models with (1) $\Omega_m = 0.3$, $\Omega_{Ch} = 0.7$; (2) $\Omega_m = 0.05$, $\Omega_{Ch} = 0.95$ and (3) $\Omega_m = 0$, $\Omega_{Ch} = 1$. We started with a fixed value of $\mathcal{M} = -3.39$ modifying this assumption accordingly while analyzing different samples.

The first class was chosen as representative of the standard knowledge of Ω_m (baryonic plus dark matter in galactic halos (Peebles & Ratra 2003)) with Chaplygin gas responsible for the missing part of closure density (the dark energy).

In the second class we have incorporated (at the level of Ω_m) the prior knowledge about baryonic content of the Universe (as inferred from the BBN considerations). Hence this class is representative of the models in which Chaplygin gas is allowed to clump and is responsible both for dark matter in halos as well as its diffuse part (dark energy).

The third class is a kind of toy model – the FRW Universe filled completely with Chaplygin gas. We have considered it mainly in order to see how sensitive the SNIa test is with respect to parameters identifying the cosmological model.

Finally, we analyzed the data without any prior assumption about Ω_m .

3.3. Results

In the first class of models best fit (with fixed value of $\mathcal{M} = -3.39$) from the sample A is ($\alpha = 1$, $A_0 = 0.96$) at the $\chi^2 = 95.8$. Sample C gives the best fit of ($\alpha = 0.95$, $A_0 = 0.95$) at the $\chi^2 = 53.6$.

In the second class Sample A gives the best fit of ($\alpha = 1$, $A_0 = 0.80$) at the $\chi^2 = 95.4$ whereas the sample C gives the best fit ($\alpha = 0.51$, $A_0 = 0.73$) at the $\chi^2 = 53.7$.

Finally, in the third class the sample A again gives the best fit of ($\alpha = 1$, $A_0 = 0.77$) at the $\chi^2 = 95.4$ whereas the sample C gives the best fit ($\alpha = 0.42$, $A_0 = 0.69$) at the $\chi^2 = 53.7$.

It should be noted, however that the fitting procedure for sample C prefers $\mathcal{M} = -3.44$ instead of $\mathcal{M} = -3.39$ as for sample A. If one takes this value the results for sample C will change respectively and then for the first class $A_0 = 1$ (at $\chi^2 = 53.5$) what means (see equation (10)) that α can be arbitrary and the problem is effectively equivalent to the model with cosmological constant. Analogously, for the second class $A_0 = 0.83$ $\alpha = 1$ (at $\chi^2 = 52.9$), while for third class $A_0 = 0.80$ $\alpha = 1$ (at $\chi^2 = 52.9$). This indicates clearly that model parameters, especially α strongly depend on the choice of \mathcal{M} .

Separately we analyzed the data without any prior assumption about Ω_m . For the sample A we obtain as a best fit (minimizing χ^2) $\Omega_m = 0.$, ($\alpha = 1, A_0 = 0.77$) at the $\chi^2 = 95.4$. For sample C assuming $\mathcal{M} = -3.39$ we obtain $\Omega_m = 0.27$, ($\alpha = 1, A_0 = 0.93$) with $\chi^2 = 53.6$ while for $\mathcal{M} = -3.44$ the best fit gives $\Omega_m = 0.$, ($\alpha = 1, A_0 = 0.80$) with $\chi^2 = 52.9$.

Using minimization procedure, based on likelihood function, joint marginalization over A_0 and α gives the following results. For the sample A we obtain $\Omega_{Ch} = 0.82$ (hence $\Omega_m = 0.18$), with the limit $\Omega_{Ch} \geq 0.76$ at the confidence level 68.3% and $\Omega_{Ch} \geq 0.69$ at the confidence level 95.4%. For the sample C we obtain (for $\mathcal{M} = -3.39$) $\Omega_{Ch} = 0.76$ (hence $\Omega_m = 0.24$), with the limit $\Omega_{Ch} \in (0.69, 0.94)$ on the confidence level 68.3% and $\Omega_{Ch} \geq 0.62$ at the confidence level 95.4%. For $\mathcal{M} = -3.44$ we obtain: $\Omega_{Ch} = 0.84$ (hence $\Omega_m = 0.16$), with the limit $\Omega_{Ch} \in (0.79, 0.98)$ on the confidence level 68.3% and $\Omega_{Ch} \geq 0.69$ at the confidence level 95.4%.

One could see that results are different for different values of the intercept \mathcal{M} in each sample. Therefore we additionally analyzed our samples marginalized over \mathcal{M} . The results are displayed in Table 1. First rows for each sample correspond to no prior on Ω_m assumed. Two fitting procedures were used: χ^2 fitting (denoted as BF) and maximum likelihood method (denoted L).

Table 2 contains the results of joint marginalization over Ω_m , A_0 and α . For sample A we obtain $\Omega_{Ch} = 0.83$ (hence $\Omega_m = 0.17$), while for sample C we obtain $\Omega_{Ch} = 0.85$ (hence $\Omega_m = 0.15$). For A_0 and α we obtain values ($\alpha = 0, A_0 = 0.83$) for sample A, while ($\alpha = 0, A_0 = 0.86$) for sample C. With the marginalization procedure we can also obtain one dimensional probability distribution function (PDF) for A_0 and α for particular class models with fixed Ω_m (Table 3).

From the above mentioned analysis we concluded that Ω_m and A_0 parameters derived from samples A and C are similar. For Ω_m fixed A_0 increases with increasing Ω_m . The estimates of α parameter are different for each of two above mentioned samples, but unfortunately errors are big. Discrepancy between the best fitting procedure and minimization procedure (based on likelihood function) increases with the number of parameters fitted. The minimization procedure seems to be more appropriate in the context of our problem.

One can see from the Table 1 that using the Knop's samples had not influenced conclusions in a significant way. However, the errors of parameter estimation decreased noticeably (see Tables 2 and 3). Minimization procedure prefers (especially for sample K3) α close to zero. The exception is the model with $\Omega_m = 0$ where $\alpha = 0.3$ and $\alpha = 0.71$ are obtained for the samples K3 and K6 respectively.

The above mentioned results for the Knop sample K3 are illustrated on figures Fig. 1 - 17. In Fig.1 we present residual plots of redshift-magnitude relations between the Einstein-de Sitter model (represented by zero line) the best-fitted Generalized Chaplygin Gas model with $\Omega_m = 0.3, \Omega_{Ch} = 0.7$ (middle curve) and the flat Λ CDM model with $\Lambda = 0.75$ and $\Omega_m = 0.25$ (Knop et al. 2003) – upper curve. One can observe that systematic deviation between Λ CDM model and Generalized Chaplygin Gas model gets larger at higher redshifts. The Generalized Chaplygin Gas model predict that high redshift supernovae should be brighter than that predicted with Λ CDM model.

Levels of constant χ^2 on the (A_0, α) plane for Generalized Chaplygin Gas model with $\Omega_m = 0.3, \Omega_{Ch} = 0.7$, marginalized over \mathcal{M} are presented in Figure 2. The figure shows preferred values of A_0 and α . Figure 3 displays confidence levels on the (A_0, α) plane for Generalized Chaplygin Gas model with $\Omega_m = 0.3, \Omega_{Ch} = 0.7$, marginalized over \mathcal{M} . This figure shows the ellipses of preferred values of $(A_0$ and $\alpha)$. Similar results for the models with $\Omega_m = 0.05, \Omega_{Ch} = 0.95$ and $\Omega_m = 0, \Omega_{Ch} = 1$ are presented in the figures 4 - 9 respectively.

Separately we repeated our analysis without prior assumptions on Ω_m . The density distribution (one dimensional PDF) for model parameters obtained by marginalization over remaining parameters of the model are presented in Figures 10-12.

Residuals (in mag) between the Einstein-de Sitter model (zero line), flat Λ CDM model – upper curve – and the best-fitted Generalized Chaplygin Gas model (without prior assumptions on Ω_m) – middle curve – are presented on Figure 13, while levels of constant χ^2 and confidence levels on the (A_0, α) plane (marginalized over \mathcal{M}) are presented on Figs. 14 and 15.

One should notice that as a best fit we obtain $\Omega_m = 0, \Omega_{Ch} = 1, A_0 = 0.85, \alpha = 1$ i.e. results are the same as for a toy model with Chaplygin gas only ($\Omega_{Ch} = 1$). Formally, we could have analyzed models with $\alpha > 1$. However, due to large error in estimation of the α parameter, it does not seem reasonable to analyze such a possibility with current supernovae data.

Levels of constant χ^2 on the (Ω_m, α) plane for Generalized Chaplygin Gas model, marginalized over \mathcal{M} and A_0 are presented on Figure 16, while confidence levels on the (Ω_m, α) plane (marginalized over \mathcal{M} , and A_0) are presented on Figure 17. This figure shows that all three model with $\Omega_{Ch} = 1$, $\Omega_{Ch} = 0.95$, and $\Omega_{Ch} = 0.7$, are statistically admissible by current Supernovae data.

The results of similar analysis obtained with Tonry/Barris sample are similar to those obtained with previous samples. For example TBII sample gives the best fit: $\Omega_m = 0, \Omega_{Ch} = 1, A_0 = 0.78, \alpha = 1$ i.e. nearly the same as in the case of K3 sample.

Joint marginalization over parameters gives the following results: $\Omega_{Ch} = 1.00$ (hence $\Omega_m = 0.0$), with the limit $\Omega_{Ch} \geq 0.79$ at the confidence level of 68.3% and $\Omega_{Ch} \geq 0.67$ at the confidence level of 95.4%. ($\alpha = 1.0, A_0 = 0.81$) with the limit $\alpha \in (0.40, 1.)$ and $A_0 \in (0.74, 0.93)$ at the confidence level of 68.3% and $\alpha \in (0.06, 1.)$ and $A_0 \in (0.70, 1.00)$ at the confidence level of 95.4%.

However with minimization procedure we find important difference between results obtained with Tonry/Barris sample and those obtained with Perlmutter and Knop samples. Minimization procedure (only except the model with fixed $\Omega_m = 0.3$) performed on Tonry/Barris data gives $\alpha = 1$. It is significantly different from the result obtained for C Perlmutter's and Knop's samples where minimization procedure preferred small values of α parameter. Also the Tonry /Barris sample preferred value of $\Omega_m = 0$ while Perlmutter and Knop samples suggested Ω_m is close to zero, what indicates that barionic component is small and in agreement with BBN.

The new Riess sample leads to the results which are similar to these obtained with Tonry/Bariss sample. However the errors in estimation of the parameters are lower. For the Gold sample, joint marginalization over parameters gives the following results: $\Omega_{Ch} = 1.00$ (hence $\Omega_m = 0.0$), with the limit $\Omega_{Ch} \geq 0.80$ at the confidence level of 68.3% and $\Omega_{Ch} \geq 0.69$ at the confidence level of 95.4%. ($\alpha = 1.0, A_0 = 0.83$) with the limit $\alpha \in (0.36, 1.)$ and $A_0 \in (0.76, 0.94)$ at the confidence level of 68.3% and $\alpha \in (0.05, 1.)$ and $A_0 \in (0.72, 1.00)$ at the confidence level of 95.4%.

As one can see from the Figure 18 the differences between the results obtained in both cases are small (however the result obtained with the full sample leads to the prediction of brighter distant supernovae than in the case with $z < 1$ SNIa.) Residuals (in mag) between the Einstein-de Sitter model (zero line), flat Λ CDM model (two upper curves: for SNIa with $z < 1$ - higher curve - and for all supernovae Ia belonging to the sample - lower curve) and the best-fitted Generalized Chaplygin Gas model (without prior assumptions on Ω_m) (middle curve) are presented on Figure 18. Figure 18 shows that most distant supernovae are actually brighter than predicted in Λ CDM model. This is in agreement with prediction of the Generalized Chaplygin Gas cosmology.

The levels of constant χ^2 and confidence levels on the (A_0, α) plane (marginalized over \mathcal{M}) are presented on Figs. 19 and 20. Fig.20 shows that confidence levels on the (A_0, α) (for Gold Sample) plane are comparable at the the 95.4% confidence level with the results obtained on the Knop's sample. However the preferred values of α are different.

3.4. Flat prior relaxed

We extended our analysis by adding a curvature term to the original GCG model. Then in equation (11) we must take into account the Ω_k term. For statistical analysis we restricted the values of the Ω_m parameter to the interval $[0, 1]$, Ω_{Ch} to the interval $[0, 2]$ and Ω_k was obtained from the constraint $\Omega_m + \Omega_{Ch} + \Omega_k = 1$. However, the cases $\Omega_k < -1$ were excluded from the analysis. The results are presented in Table IV and V.

In the model without prior assumptions on Ω_m we obtain with Knop's sample $\Omega_k = -0.19$ as a best fit, while with maximum likelihood method prefers $\Omega_k = -0.60$. However, the model with priors on Ω_m or Ω_{Ch} the maximum likelihood method prefers the universe much "closer" to the flat one. Specifically, for the "toy" model with Chaplygin Gas only one gets $\Omega_k = 0.10$ and $\Omega_k = 0.05$ for the model with baryonic content only i.e. $\Omega_m = 0.05$. One should emphasize that even though we allowed $\Omega_k \neq 0$ the preferred model of the universe is nearly a flat one, which is in agreement with CMBR data. It is an advantage of our GCG model as compared with Λ CDM model where in Perlmutter et al. (1999) high negative value of Ω_k was obtained as a best fit, although zero value of Ω_k was statistically admissible. In order to find the curvature of the Universe they additionally used the data from CMBR and extragalactic astronomy.

Density distribution functions (one dimensional PDF) for model parameters obtained by marginalization over remaining parameters of the model are presented in Figures 21-25. For Ω_k we obtain the limit $\Omega_k \in (-0.98, -0.22)$ at the confidence level 68.3% and $\Omega_k \in (-1, 0.23)$ at the confidence level 95.4%. For α and A_0 parameters we obtain the following results: $\alpha = 0$. and $A_0 = 0.89$ with the limit $\alpha \in (0, 0.64)$ and $A_0 \in (0.82, 1)$ at the confidence level 68.3% and $\alpha \in (0., 0.95)$ and $A_0 \in (0.73, 1.)$ at the confidence level 95.4%. For the density parameter Ω_{Ch} we obtain the limit $\Omega_{Ch} \in (0.87, 1.51)$ at the confidence level 68.3% and $\Omega_{Ch} \in (0.61, 1.79)$ at the confidence level 95.4%. For the density parameter Ω_m we obtain the limit $\Omega_m < 0.29$ at the confidence level 68.3% and $\Omega_m < 0.53$ at the confidence level 95.4%.

Our main result is that the preference of the nearly flat universe is confirmed with the new Riess sample. In the model without a prior assumption on Ω_m we obtain $\Omega_k = -0.12$ as a best fit, with the Gold sample while maximum likelihood method prefers $\Omega_k = -0.32$ i.e the Gold sample gives even "more flat" universe than Knop's sample. The models with priors on Ω_m give also very similar results when we analyse Knop and Riess samples. One can see that estimation of other models parameters give similar result for both samples only with exception for parameter α . Specifically, for the "toy" and "baryonic" models the maximum likelihood method prefers the universe with non zero parameter α like for "flat universe". One can see that, with flat prior relaxed, when we analyse the Gold sample, the errors in

estimation of the model parameter significantly decrease with comparison to the case of the Knop sample.

4. Generalized Chaplygin Gas model in perspective of SNAP data

In the near future the SNAP mission is expected to observe about 2000 SN Ia supernovae each year, over a period of three years ¹. Therefore it could be possible to discriminate between various cosmological models since errors in the estimation of model parameters would decrease significantly. We tested how a large number of new data would influence the errors in estimation of model parameters. We assumed that the Universe is flat and tested three classes of cosmological models. In the first Λ CDM model we assumed that $\Omega_m = 0.25$, and $\Omega_\Lambda = 0.75$ and $\mathcal{M} = -3.39$ (Knop et al. 2003). Second class was representative of the so called Cardassian models (Freese & Lewis 2002) with parameters $\Omega_m = 0.42$, $\Omega_{card} = 0.52$ and $n = -0.77$ as obtained in (Godłowski, Szydlowski & Krawiec 2004). Let us note, that technically i.e. at the level of tests like the Hubble diagram Cardassian models are equivalent to quintessence models. The difference is in the underlying philosophy: quintessence assumes exotic dark energy component with hydrodynamical equation of state in ordinary FRW model while the Cardassian Universe assumes modification of the Friedman equation (which can be either due to exotic matter component or due to modification of gravity law). The last model is Generalized Chaplygin Gas Model with parameters obtained in the present paper as best fits for the K3 sample ($\Omega_m = 0$, $A_0 = 0.85$, $\alpha = 1$). These values are in agreement with results of the analysis performed on Tonry/Barris and Riess samples. Alternatively, we also test the Generalized Chaplygin Gas Model with small value of α parameter suggested by analysis of the Perlmutter and Knop samples ($\Omega_m = 0$, $A_0 = 0.76$, $\alpha = 0.40$). For three above mentioned models we generated a sample of 1915 supernovae (Samples X1,X2,X3a,X3b respectively) in the redshift range $z \in [0.01, 1.7]$ distributed according to predicted SNAP data (see Tab I of Alam et al. (2003)). We assumed Gaussian distribution of uncertainties in the measurement of m and z . The errors in redshifts z are of order $1\sigma = 0.002$ while uncertainty in the measurement of magnitude m is assumed $1\sigma = 0.15$. The systematic uncertainty is $\sigma_{sys} = 0.02$ mag at $z = 1.5$ (Alam et al. 2003). Hence one can assume that $\sigma_{sys}(z) = (0.02/1.5)z$ in first approximation. For such generated sample we repeated our analysis. The result of our analysis is presented on figures Fig.26-29. On these figures we present confidence levels on the plane (A_0, α) for sample of simulated SNAP data. The figures show the ellipses of preferred values of A_0 and α . It is easy to see that with the forthcoming SNAP data it will be possible to discriminate between predictions of Λ CDM

¹<http://www-supernova.lbl.gov>, <http://snfactory.lbl.gov>

and GCG models. With Cardassian Model the situation is not so clear, however (see Fig 27 and 28). Note that if $\alpha \simeq 0.4$ as suggested by analysis of Perlmutter sample C, (see also: Makler, de Oliveira & Waga 2003, Avelino et al. 2003, Fabris, Gonnçaves & de Souza 2002, Collistete et al. 2003) then it will be possible to discriminate between model with Chaplygin gas and Cardassian model (see Fig 27 and 29). Moreover, it is clear that with the future SNAP data it would be possible to differentiate between models with various value of α parameter. This is especially valuable since all analyses performed so far have had weak sensitivity with respect to α .

5. Conclusions

It is apparent that Generalized Chaplygin Gas models have brighter supernovae at redshifts $z > 1$. Indeed one can see on respective figures (Figs 1, 4, 7, 13) that systematic deviation from the baseline Einstein de Sitter model gets larger at higher redshifts. This prediction seems to be independent of analysed sample.

We obtained that the estimated value of A_0 is close to 0.8 in all considered models with exception the model class (1) ($\Omega_m = 0.3$) when $A_0 > 0.95$. Extending our analysis by relaxing the flat prior lead to the result that even though the best fitted values of Ω_k are formally non-zero, yet they are close to the flat case. It should be viewed as an advantage of the GCG model since in similar analysis of Λ CDM model in Perlmutter et al. (1999) high negative value of Ω_k were found to be best fitted to the data and independent inspiration from CMBR and extragalactic astronomy has been invoked to fix the curvature problem. Another advantage of GCG model is that in a natural way we obtained the conclusion that matter (baryonic) component should be small what is in agreement with prediction from BBN (Big Bang Nucleosynthesis). Both estimations of A_0 , Ω_k and Ω_m are independent of the sample used in our analysis.

Our results suggest that SNIa data support the Chaplygin gas (i.e. $\alpha = 1$) scenario when the χ^2 best fitting procedure is used. The minimization procedure performed on Tonry/Barris and Riess data gives also $\alpha = 1$ (only except the model with fixed $\Omega_m = 0.3$). However, the maximum likelihood fitting with Knop et al.'s sample prefers, quite unexpectedly, a small value of α or even $\alpha = 0$, i.e. the Λ CDM scenario. Please note that small value of α is in agreement with the results obtained from CMBR (de Bernardis et al. 2000 Benoit et al. 2003, Hinshaw et al. 2003, Bento, Bertolami & Sen 2002, Amendola et al. 2003) and with the recent analysis of Zhu (2004) who, using combined data of X-ray gas mass fraction of the galaxy cluster, FR IIB radiogalaxies and combined sample Perlmutter et al. (1998) and Riess et al. (1998, 2001), suggested that α could be even less than 0. The results are

dependent both on the sample chosen and on the prior knowledge of \mathcal{M} in which the Hubble constant and intrinsic luminosity of SNIa are entangled. Moreover the observed preference of A_0 values close to 1 means that the α dependence becomes insignificant (see equation (10)). It is reflected on one dimensional PDFs for α which turned out to be flat meaning that the power of the present supernovae data to discriminate between various Generalized Chaplygin Gas models (differing by α) is weak.

However, we argue that with future SNAP data it would be possible to differentiate between models with various value of α parameter. Residual plots indicate the differences between Λ CDM and Generalized Chaplygin Gas cosmologies at high redshifts. Therefore one can expect that future supernova experiments (e.g. SNAP) having access to higher redshifts will eventually resolve the issue whether the dark energy content of the Universe could be described as a Chaplygin gas. The discriminative power of forthcoming SNAP data has been illustrated on respective figures (Fig.26-29) obtained from the analysis on simulated SNAP data.

6. Acknowledgements

We thank dr Barris and dr Riess for explanation of details of their SNIa samples. MS was supported by KBN grant no 2P03D00326

REFERENCES

- Alam U. et al., *Mon.Not. Roy. Astron. Soc.* **344**, 1057, 2003
- Alcaniz J.S., Jain D., Dev A., *Phys. Rev. D* **67**, 043514, 2003
- Alcaniz J.S., and Lima J.A.S., astro-ph/0308465, 2003
- Amendola L., Finelli F., Burigana C., Carturan D., *JCAP* **0307**, 5, 2003
- Avelino P.P., Beça L.M.G., de Carvalho J.P.M., Martins C.J.A.P., Pinto P., *Phys. Rev. D* **67**, 023511, 2003
- Barris B. J. et al. 2003 astro-ph/0310843
- Bean R., Doré O., *Phys. Rev. D* **68**, 023515, 2003
- Benoit A., et al., *Astron.Astrophys.* **399**, L25-L30, 2003

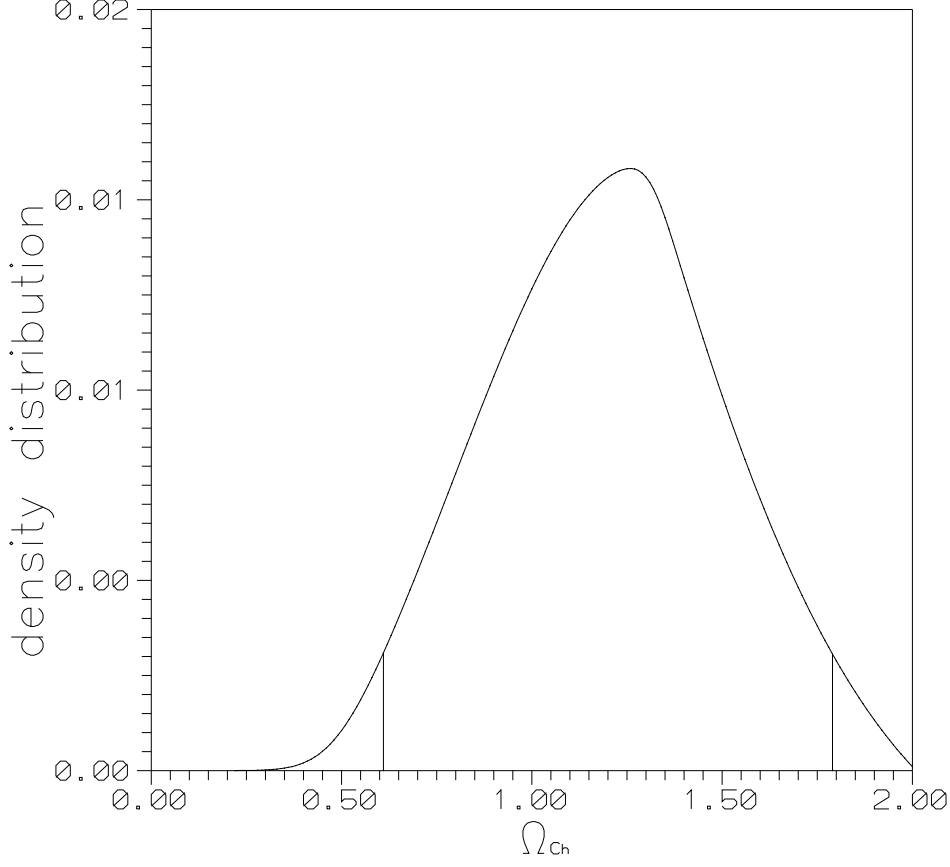


Fig. 21.— The density distribution (one dimensional PDF) for Ω_{Ch} obtained from sample K3 by marginalization over remaining parameters of the model. We obtain the limit $\Omega_{Ch} \in (0.61, 1.79)$ at the confidence level 95.4%. (Non-flat GCG model.)

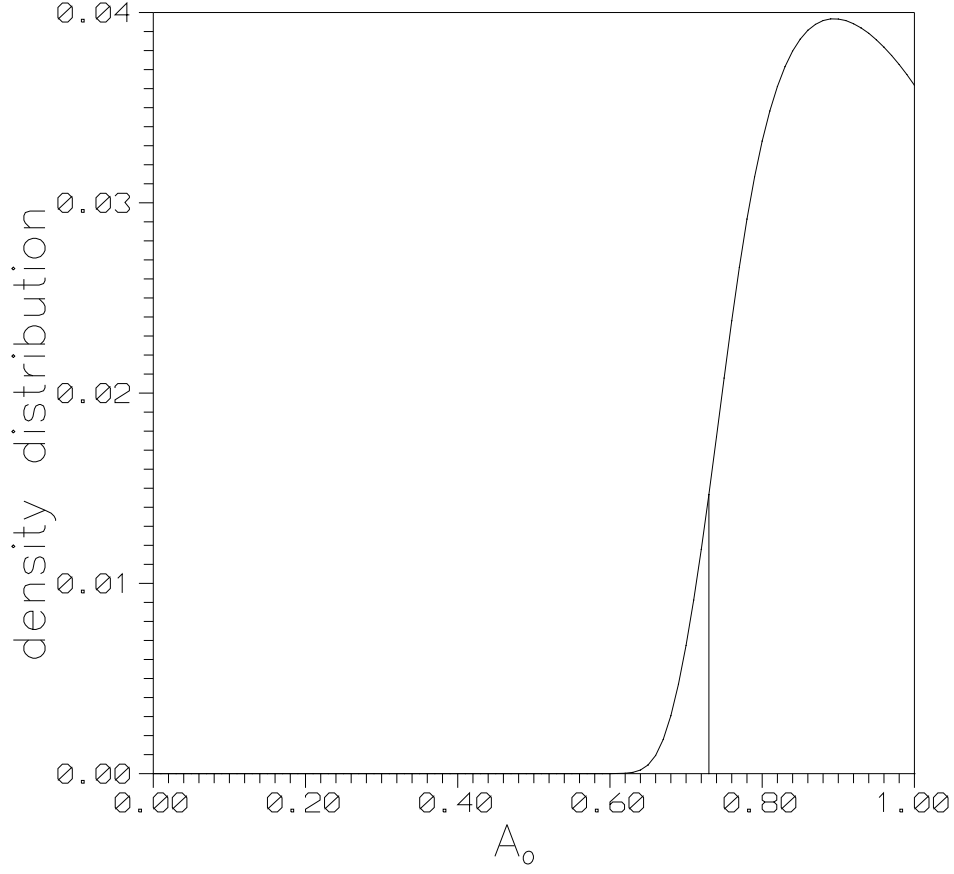


Fig. 22.— The density distribution (one dimensional PDF) for A_0 obtained from sample K3 by marginalization over remaining parameters of the model. We obtain the limit $A_0 \in (0.73, 1)$ at the confidence level 95.4%. (Non-flat GCG model.)

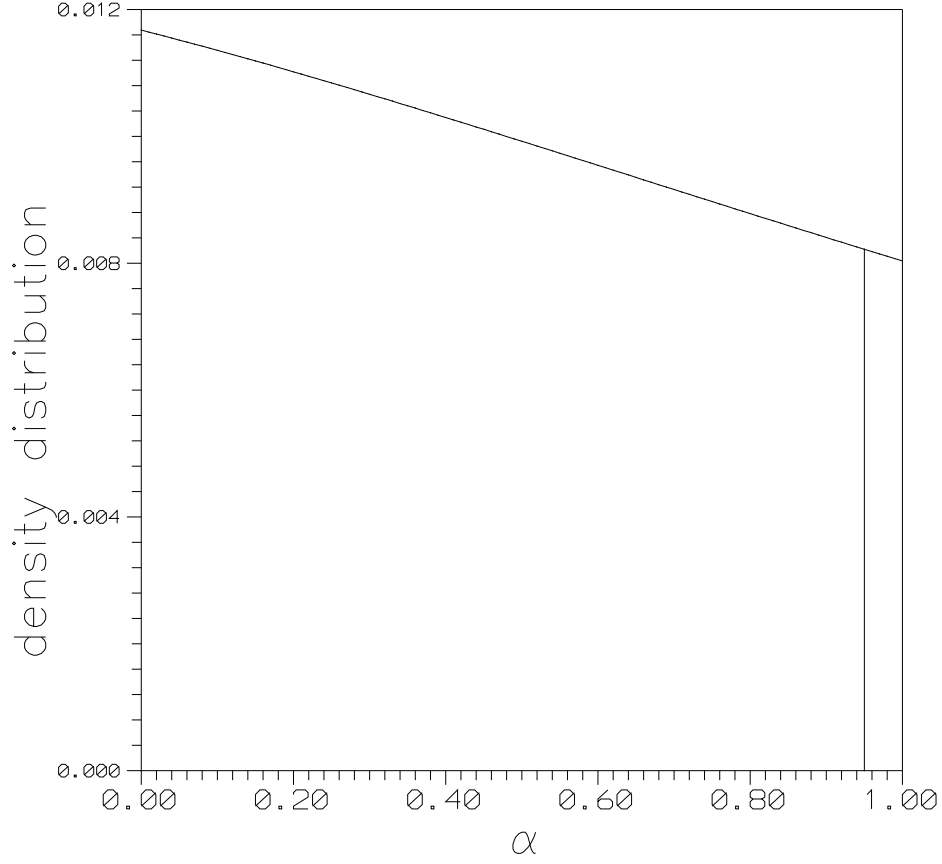


Fig. 23.— The density distribution (one dimensional PDF) for α obtained from sample K3 by marginalization over remaining parameters of the model. We obtain the limit $\alpha < 0.95$ at the confidence level 95.4%. (Non-flat GCG model.)

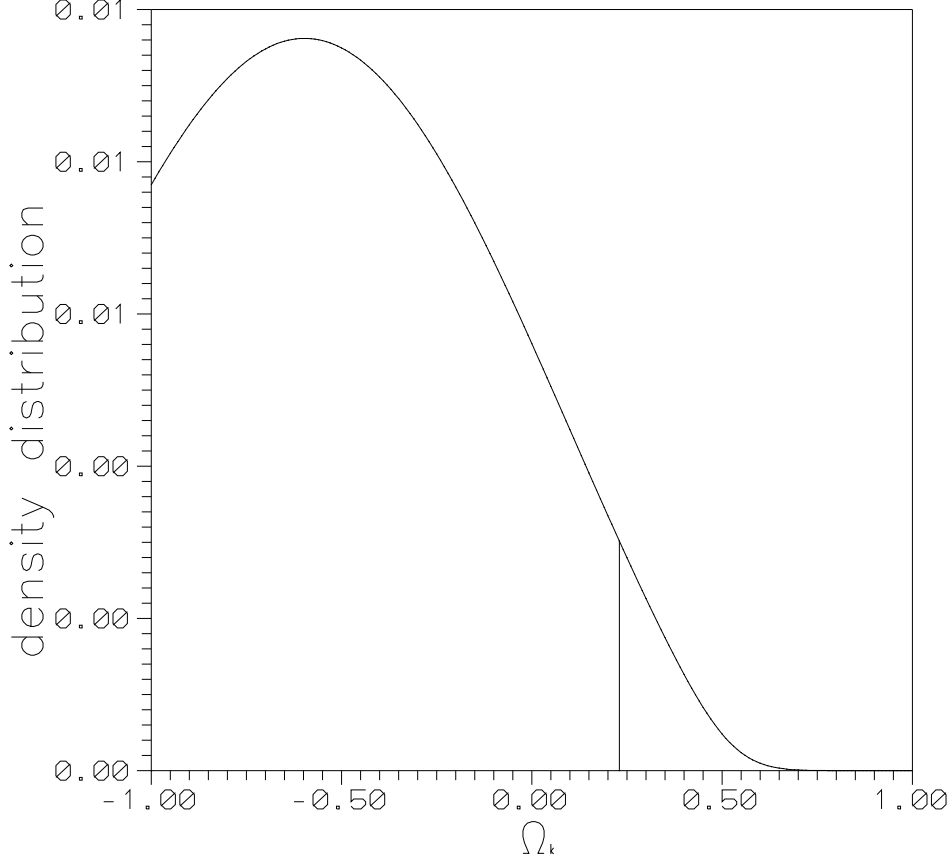


Fig. 24.— The density distribution (one dimensional PDF) for Ω_k obtained from sample K3 by marginalization over remaining parameters of the model. We obtain the limit $\Omega_k \in (-1, 0.23)$ at the confidence level 95.4%. (Non-flat GCG model.)

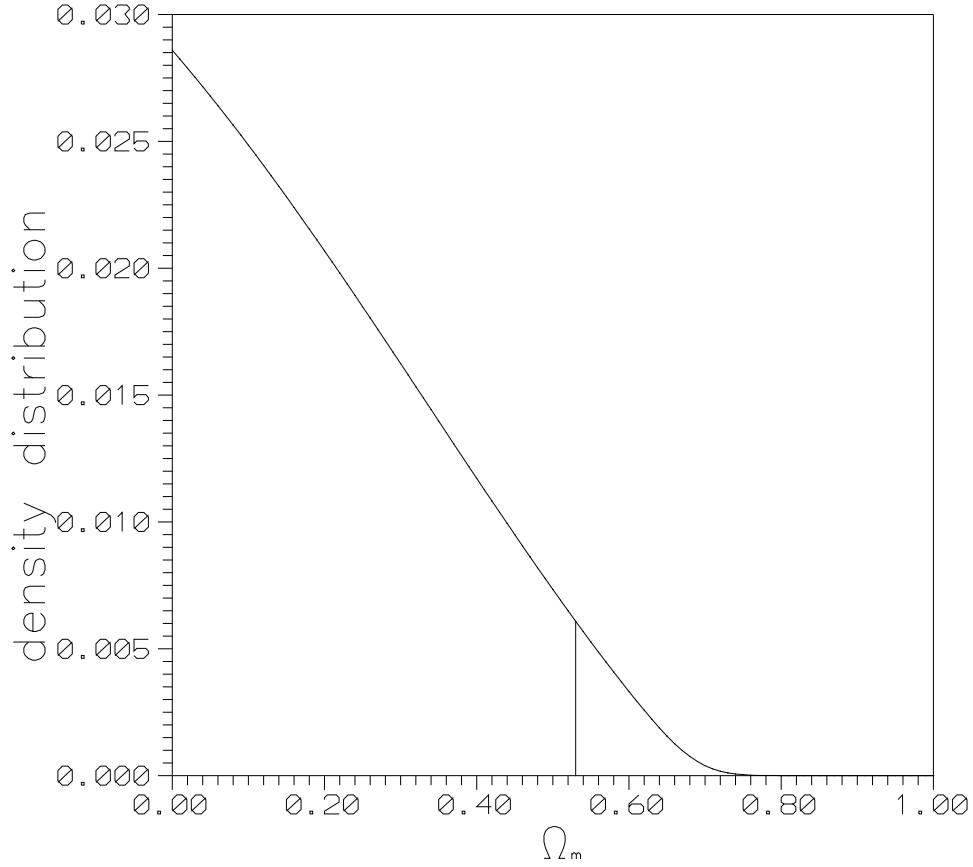


Fig. 25.— The density distribution (one dimensional PDF) for Ω_m obtained from sample K3 by marginalization over remaining parameters of the model. We obtain the limit $\Omega_m \in (0, 0.53)$ at the confidence level 95.4%. (Non-flat GCG model.)

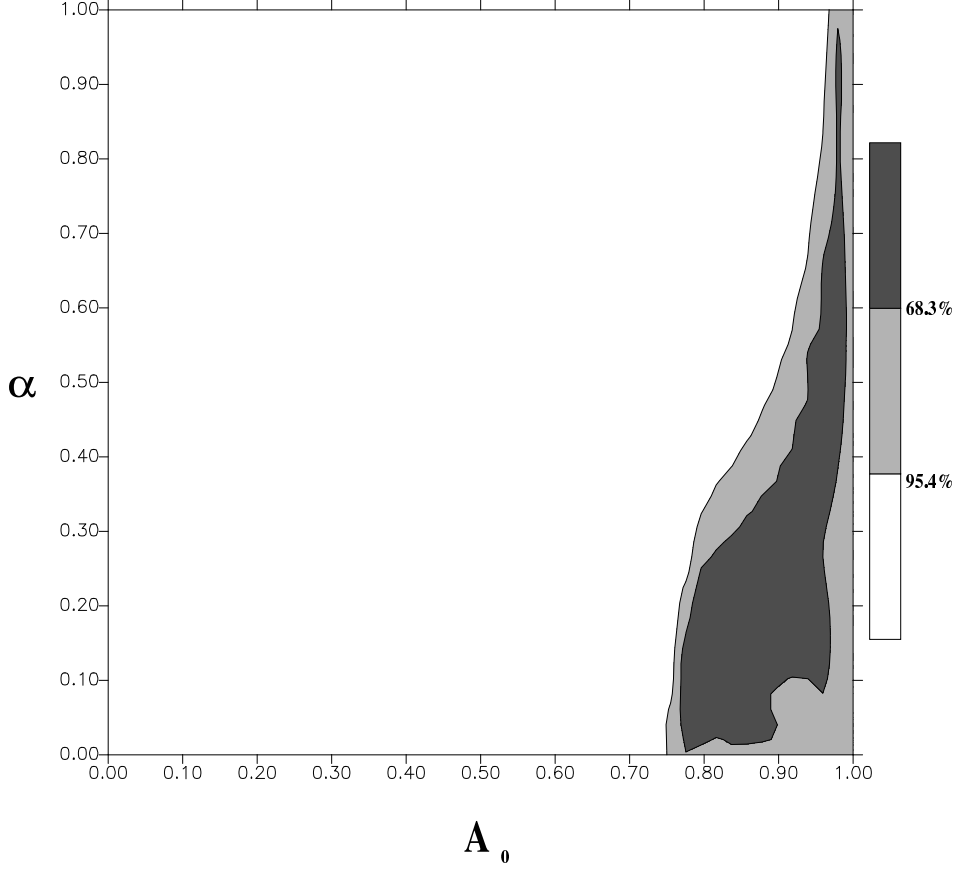


Fig. 26.— Confidence levels on the plane (A_0, α) for sample X1 (Λ CDM model) of simulated SNAP data, marginalized over Ω_m . The figure shows the ellipses of preferred values of A_0 and α .

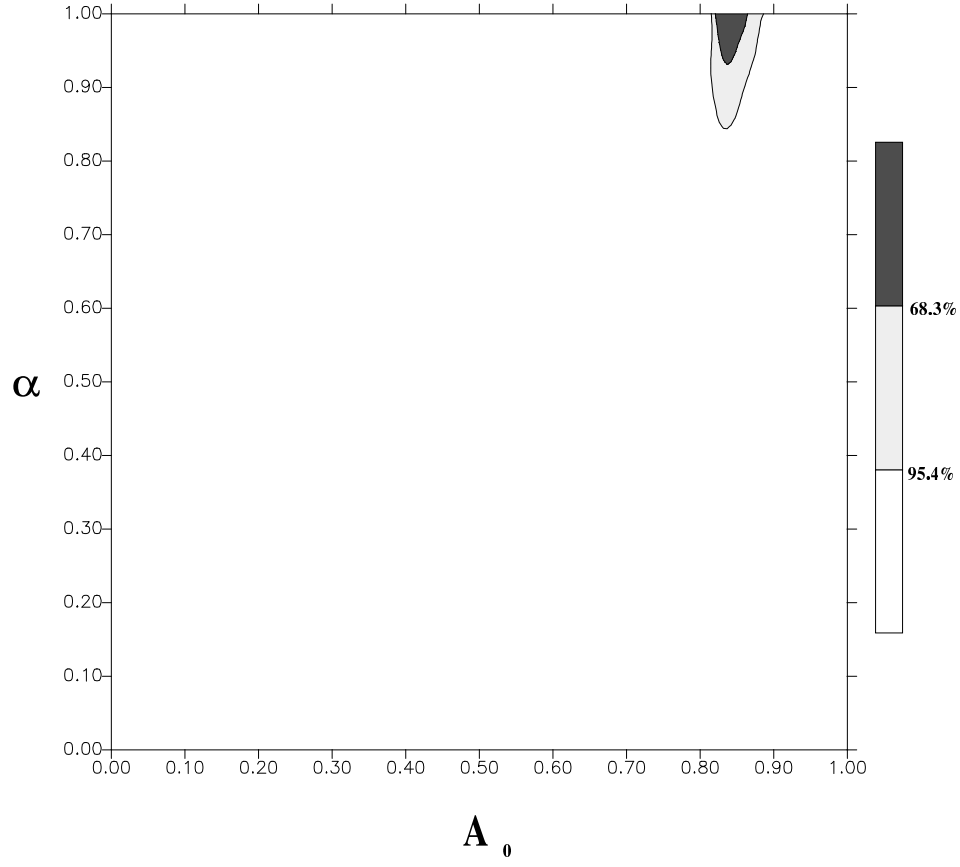


Fig. 27.— Confidence levels on the plane (A_0, α) for sample X2 (Cardassian model) of simulated SNAP data, marginalized over Ω_m . The figure shows the ellipses of preferred values of A_0 and α .

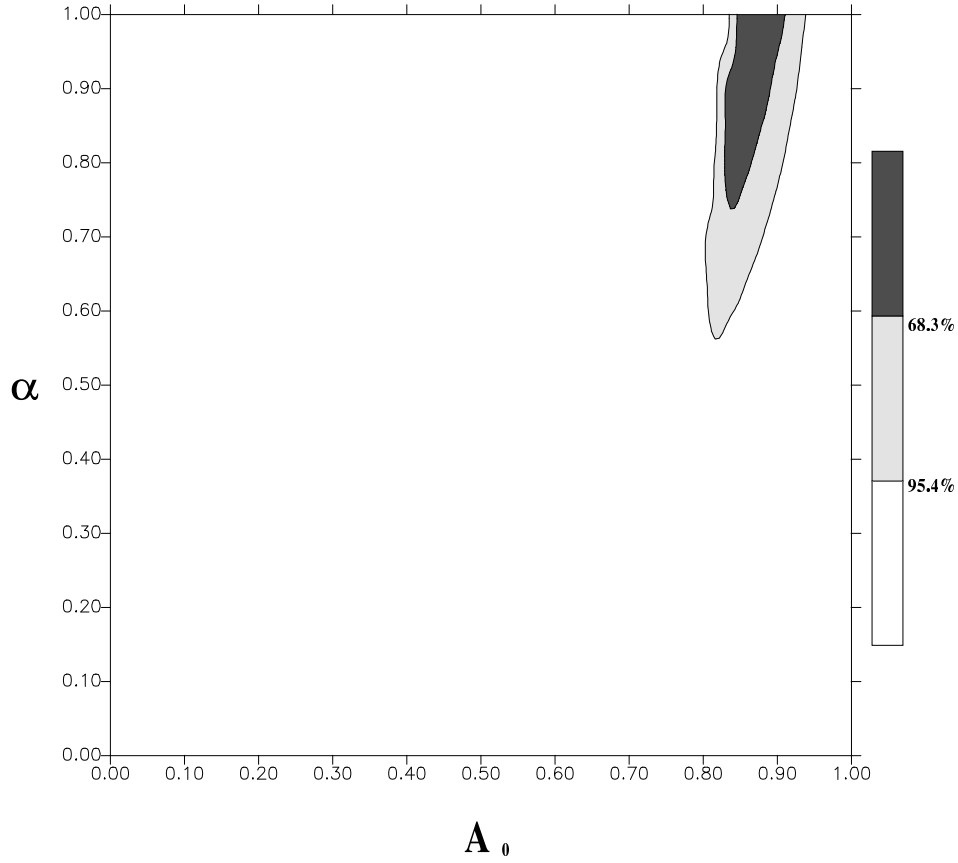


Fig. 28.— Confidence levels on the plane (A_0, α) for sample X3a (Generalized Chaplygin Gas model) of simulated SNAP data ($\Omega_m = 0$, $A_0 = 0.85$, $\alpha = 1.$), marginalized over Ω_m . The figure shows the ellipses of preferred values of A_0 and α .

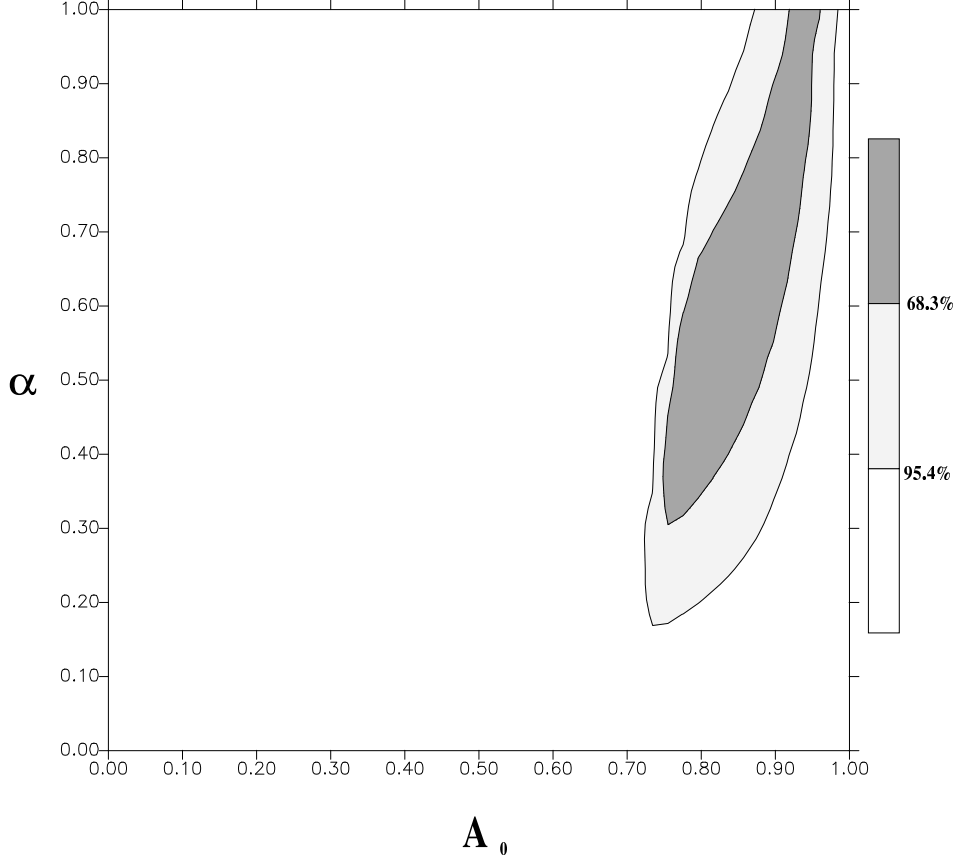


Fig. 29.— Confidence levels on the plane (A_0, α) for sample X3b (Generalized Chaplygin Gas model) of simulated SNAP data ($\Omega_m = 0$, $A_0 = 0.76$, $\alpha = 0.49$), marginalized over Ω_m . The figure shows the ellipses of preferred values of A_0 and α .

- Bento M.C., Bertolami O., Sen A.A., *Phys.Rev. D* **66**, 043507, 2002
- Bento M.C., Bertolami O., Sen A.A., *Phys.Rev. D* **67**, 063003, 2003
- Bento M.C., Bertolami O., Sen A.A., *Phys.Lett. B* **575**, 172–180, 2003
- Bertolami O., Sen A.A., Sen S., Silva P.T., astro-ph/0402387
- deBernardis P. et al., *Nature* **404**, 955, 2000
- Biesiada M., *Acta Phys. Polon.B* **34**, 5423–5432, 2003
- Bilic N., Lindenbaum R.J., Tupper G.B., Viollier R.D., astro-ph/0307214
- Bordemann M., Hoppe J., *Phys. Lett. B* **317**, 315, 1993
- Caldwell R.R., Dave R., Steinhardt P.J., *Phys. Rev. Lett.* **75**, 2077, 1995
- Carturan D., Finelli F., 2002 astro-ph/0211626v1
- Carturan D., Finelli F., *Phys.Rev. D* **68**, 103501, 2003
- S.Chaplygin, *Sci. Mem. Moscow Univ. Math* **21**, 1, 1904
- Chiba T., Sugiyama N., Nakamura T., *M.N.R.A.S.* **301**, 72, 1998
- Choudhury T.R., Padmanabhan T. AA accepted 2004 astro-ph/0311622
- Collistete Jr. R., Fabris J.C., Gonçalves S.V.B., de Souza P.E., astro-ph/0303338
- Cunha J.V., Lima J.A.S., Alcaniz J.S., astro-ph/0306319
- Dev A., Alcaniz J.S., Jain D., *Phys. Rev. D* **67**, 023515, 2003
- Fabris J.C., Gonçalves S.V.B., de Souza P.E., *Gen.Relat.Grav.* **34**, 53, 2002
- Freese K., Lewis M., *Phys. Lett. B* **540**, p1 2002
- Frieman J., Hill C., Stebbins A., Waga I., *Phys. Rev. Lett.* **75**, 2077, 1995
- Garousi M.R., *Nucl. Phys.* **B584**, 284, 2000
- Godłowski W., Szydlowski M., Krawiec A., *Astrophys.J* **605**, 599, 2004, astro-ph/0309569
- Gorini V., Kamenshchik A., Moschella V., Pasquier V., gr-qc/0403062, 2004
- Hinshaw G. et al. [WMAP collaboration], 2003, ApJ submitted; astro-ph/0302217

- R.Jackiw *A particle field theorist's lecture on supersymmetric, non abelian dynamics and D-branes*;report *MIT-CPT 3000* physics/0010042
- Kamenshchik A., Moschella V., Pasquier V., *Phys.Lett. B* **511**, 265 2001
- Kolda C., Lyth D., *Phys.Lett. B* **458**, 197, 1999
- Knop R. A. et al. , *Astrophys.J* **598**, 102, 2003; astro-ph/0309368
- Makler M., de Oliveira S.Q., Waga I., *Phys.Lett. B* **555**, 1, 2003
- Maor I., Brustein R., Steinhardt P.J., *Phys.Rev.Lett.* **86**, 6-9 (2001)
- Multamaki T., Manera M., Gaztanaga E., astro-ph/0307533
- Ogawa N., *Phys.Rev. D* **62**, 085023, 2000
- Peebles P. J. E., Ratra B., *Rev. Mod. Phys.***75**, 559 2003
- Perlmutter S., Aldering G., Goldhaber G., et al., *Astrophys.J* **517**, 565, 1999
- Randall L., Peebles P.J.E., *Phys.Rev.Lett* **83**, 4690, 1999
- Ratra B., Peebles P.J.E., *Phys.Rev.D* **37**, 3406, 1988
- Riess A., Filipenko A.V., Challis P., et al., *Astron.J* **116**, 1009, 1998
- Riess A., Nugent P.E., Gilliland R.L., et al., *ApJ* **560**, 49, 2001
- Riess A. G. et al. 2004 astro-ph/0402512
- Sen A., *JHEP* **0204**, 048, 2002
- Silva P.T., Bertolami O., astro-ph/0303353
- Szydlowski M., Czaja W. *Phys.Rev. D* **69**, 023506, 2004
- Tonry J.L., et al., *Astrophys.J* **594**, 1, 2003
- Turner M.S., White M., *Phys.Rev.D* **56**, 4439 (1997)
- Turner M., *Astrophys.J* **576**, L101-L104, 2002
- Weller J., Albrecht A., *Phys.Rev.Lett.* **86**, 1939-1942 (2001)
- Williams B. F. et al. 2003 astro-ph/0310432

Zhu Z. H., *Astron.Astrophys.* **423**, 421, 2004